FUNDAMENTALS OF HYPERSONIC FLOW - AEROTHERMODYNAMICS

D. G. Fletcher
von Karman Institute, Belgium

1. Introduction

To aid in understanding the different topics discussed in the current Lecture Series and to provide background material for interested participants who may not have specialized training in this field, a brief summary of the fundamental attributes of hypersonic flows is given. Many of the topics that are introduced in this section will be elaborated further in contributions related to specific subjects related to sustained hypersonic flight. The differences between the thermal and chemical aspects of hypersonic flow and supersonic flow are therefore highlighted. The age of some of the figures used in the subsequent discussion reflect the fact that the problems of hypersonic flight are not newly discovered!

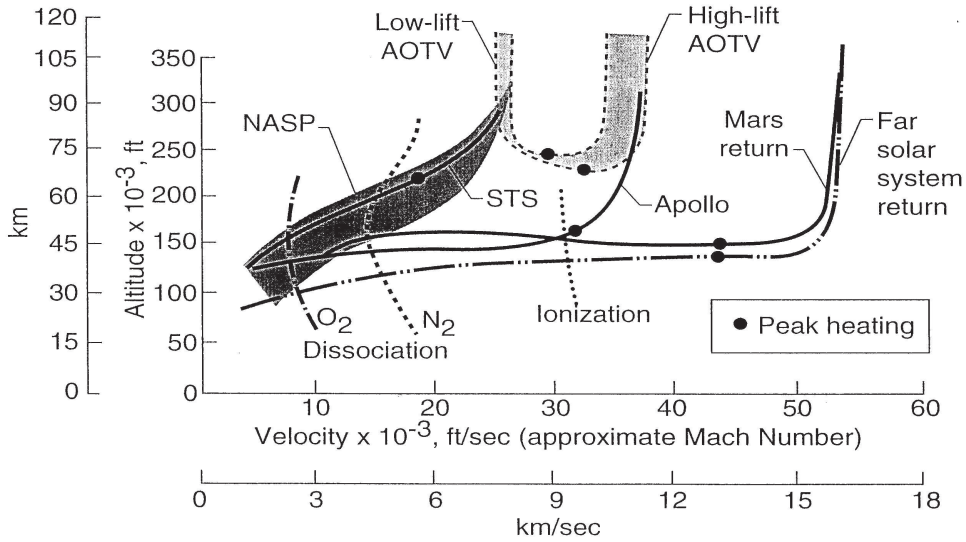

Fig. 1.1 Flight trajectories for different hypersonic vehicles comparing sustained atmospheric flight with re-entry.

The hypersonic flight regime includes atmospheric entry and re-entry, ground testing, and flight for both powered and unpowered vehicles. In the present Lecture Series, the main interest is on sustained and controlled hypersonic flight, whether for military or civil transport application. Even though it is not currently certified for flight, there is one operational hypersonic vehicle: the space shuttle of NASA. At least 20 years before the development of the shuttle a significant activity in hypersonic flight research was conducted by the US Air Force in their X-15 program. This vehicle has reached a flight Mach number of 6.7 on its final flight, which also used to test a hypersonic ramjet engine. Direct shock impingement on the pylon holding a dummy engine caused severe heating and structural damage, and this was one of many lessons learned from the program. Owing to the design of the X-15, it was not capable of long-duration powered flight, but it provided a great deal of information on technical problems that still remain a serious

Paper presented at the RTO AVT Lecture Series on "Critical Technologies for Hypersonic Vehicle Development", held at the von Kármán Institute, Rhode-St-Genèse, Belgium, 10-14 May, 2004, and published in RTO-EN-AVT-116.

obstacle to the development of new hypersonic vehicles. It is still astonishing to look back on the rapid development of high speed flight in the years after the second World War. The challenge is to build on this experience, and to accomplish the development of a new generation of flight vehicles. To put sustained hypersonic flight in context, current and proposed hypersonic vehicle trajectories are compared in Fig. 1.1.

Although un-powered hypersonic vehicles are not the topic of the present Lecture Series it is important to note that there have been many more successful developments of these types of vehicle, predominantly in the reentry of manned and unmanned spacecraft of Russian, American, and European origin into earths atmosphere. For example, the Apollo reentry conditions were 53 km altitude, 11 km/s velocity, 270 K temperature, and speed of sound 338 m/s which gave a reentry Mach number of M = 32.5. There have also been a number of missions to other planets (more vehicles going to these planets than have been developed for sustained hypersonic flight within the atmosphere) and the entry speeds into those atmospheres have been even greater. A recent, noteworthy example of this was the Galileo probe to Jupiter that was designed to enter the Jovian atmosphere at 60 km/s at an altitude of 1000 km. At this altitude, the temperature is approximately 800 K, and the atmosphere was assumed to consist of H_2 and He at a mixture of (89:11) by mass. Therefore, the entry Mach number was about 28 for this mission. Even though the entry speed was greater than that of the Apollo reentry, the Mach number is lower owing to the greater value of the sound speed in the hydrogen-helium atmosphere.

Clearly, Mach number is not the only parameter that must be considered for hypersonic flight; in fact, it is often only of secondary importance. In Earth's atmosphere for example, the temperature of the outer atmosphere is quite low, so the sound speed is lower than at sea level and higher Mach numbers can be achieved there at lower speeds. A better measure is the speed itself, since it can also give an indication of the kinetic energy involved in the trajectory. For hypersonic craft, the flight enthalpy can usually be estimated very quickly from the speed as $h = u^2/2$. As will be discussed later, the amount of aerothermodynamic heating that the vehicle must deal with is linearly dependent on the kinetic energy of the vehicle. This is a very important aspect of hypersonic flight through planetary atmospheres. The vehicle encounters such severe heating that a significant part of the design and development effort is concerned with providing sufficient protection of the payload without using all payload capacity for doing this! Other general characteristics of hypersonic flows are that molecules behind a high-velocity shock wave become vibrationally excited, partially or completely dissociated depending on their bond energy, and, at very high speeds, partially ionized. These aspects of hypersonic flow are typically called "real gas" effects. To clarify what is meant by "real-gas effects", it is useful to bear in mind the following definitions:

Thermally Perfect Gas: A thermally perfect gas is one that obeys the ideal gas equation of state,

$$p = \rho RT \quad .$$

From compressible flow theory, this relationship implies that internal energy and enthalpy depend only on temperature.

Calorically Perfect Gas: A calorically perfect gas has constant values of specific heat, independent of temperature.

Perfect, or Ideal, Gas: This designation refers to a gas that is both thermally and calorically perfect.

Thermal Equilibrium: A single temperature can be used to describe the different molecular internal energy modes (which are described in detail below). This single temperature describes the energy modes of all molecules and it is the same as the temperature of the surroundings.

Chemical Equilibrium: All chemical reactions are in balance and the system does not spontaneously undergo any change in chemical composition, no matter how slow. For this situation the distribution of species is uniquely described by two thermodynamic variables, such as density and temperature.

Note that a "real gas" is not defined, since it is used by fluid dynamicists to describe all of the situations that are not perfect. However, it will be shown later that the most important real, or imperfect gas effects for hypersonic flight in earth atmosphere are caloric.

As in other flow regimes, non-dimensional parameters are used to describe hypersonic flow. Most of these paramaters are encountered in other flow domains, including subsonic and supersonic flow, but they are summarized here for convenience:

1. Reynolds, $Re = VL/\nu$. This can be taken as a measure of the viscous flow time over the mean flow time.
2. Mach, $M = V/a$. This is a measure of the flow speed relative to the acoustic propagation speed.
3. Knudsen, $Kn = \lambda/L (= M/Re)$. This an indication of the collision path length relative to a flow scale
4. Prandtl, $Pr = \nu/\kappa$. A measure of the thermal diffusion time relative to the viscous diffusion time.
5. Schmidt, $Sc = \nu/D$. This is an indication of the species diffusion time relative to the viscous diffusion time.
6. Eckert, $E = u^2/h$. Indicates the relative magnitudes of kinetic and thermal energy for the flow.
7. Damkohler, $Da = \tau_f/\tau_c$. This dimensionless parameter is the ratio of the characteristic flow time (such as a residence time) to a characteristic chemical reaction time. When it is very large, the chemical reactions can be complete, and the flow will likely be in chemical equilibrium. When it is very small, the chemical reactions will not be complete and the flow chemistry is considered to be frozen. For hypersonic flow, in contrast to other flow regimes, the Damkohler number plays an important role, determining whether or not the flow is in equilibrium.

To relate the discussion of thermodynamic and gasdynamic considerations to applications of interest it is useful to consider first general high-temperature gas effects that are encountered in the hypersonic flight of a typical vehicle, as illustrated in Fig. 1.2 (it should be noted that apart from compressibility, none of the attributes mentioned below are found in the supersonic flow regime.

Caloric and Chemical Effects: The atmospheric composition behind a normal shock ahead of a hypersonic vehicle will differ greatly from the atmosphere ahead of the shock. Diatomic molecules will be vibrationally excited and dissociated to some extent,

and the resulting atoms and remaining molecules can be partially ionized. Thus, for the remaining post-shock molecules, the assumption that they behave as calorically perfect gases is no longer valid. Within a vehicle boundary layer, there is sufficient viscous dissipation to also affect the stream chemistry and this can lead to chemically reacting boundary layers. As specific heats are no longer constant owing to vibrational excitation and chemical reaction, their ratio $\gamma = c_p/c_v$ is also no longer constant, but also depends on the temperature. For air, this begins at around 800 K.

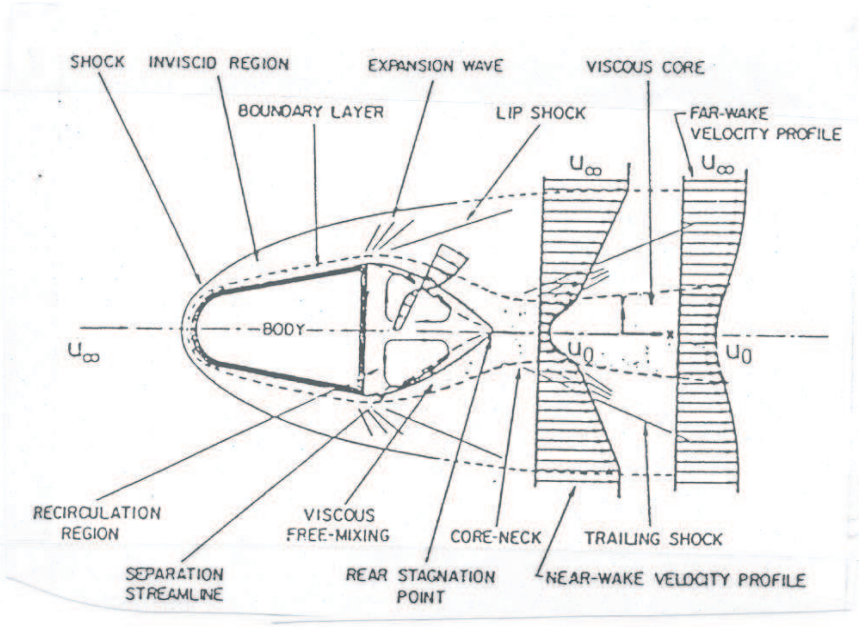

Fig. 1.2 Features of hypersonic flow around a blunt-nosed vehicle.

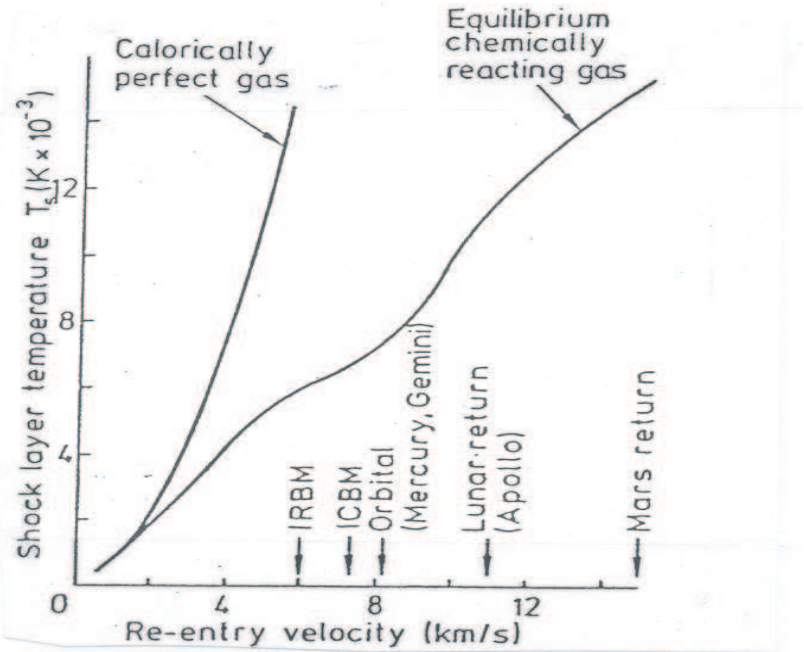

Fig. 1.3 Post shock temperature of a re-entry vehicle at 52 km and 1 atm pressure.

The amount of energy driving chemical reactions is significant. As an example, consider Fig 1.3, which shows the shock-layer temperature as a function of re-entry velocity at

an altitude of 52 km. The line to the left is the temperature of a calorically perfect gas. Specific heat is constant and the kinetic energy is simply converted into thermal energy assuming equilibrium. On the right is the equilibrium temperature for a chemically reacting gas. Some of the kinetic energy is converted into chemical energy, thereby reducing the post-shock temperature. Depending on the material that comprises the vehicle thermal protection system, the atomic flux to the surface can result in significant extra heating through the mechanism of surface-catalyzed recombination (which releases energy as heat on the surface).

Aerodynamic Forces: Another important aspect of hypersonic flight is that the variation in the ratio of specific heats, γ, can significantly affect the pressure distribution over a vehicle or its control surfaces. This is because γ, which is also the isentropic exponent, directly influences the rate of expansion or compression of the flow. This can manifest itself in the setting of control surface angles, or even in the trim angle of attack for a vehicle, which can be larger than that predicted for the perfect gas value of γ by 2 to 4 degrees. This was actually observed during the first Shuttle reentry. A calculation had been done of the pressure distribution along the windward side of the vehicle for a non-reacting, perfect gas boundary layer ($\gamma = 1.4$) and for a chemically reacting boundary layer. The calculations are shown in Fig. 1.4, and they look very similar. However, we can see a small but consistent difference in pressure values that are slightly higher for the forward region and lower in the aft region for the reacting case. When integrated over the vehicle surface, this produces a net moment that provided additional pitch-up to the Shuttle nose and required manual control to override. Note that other explanations have also been given for this, which illustrates how difficult it is to isolate interacting physical phenomena.

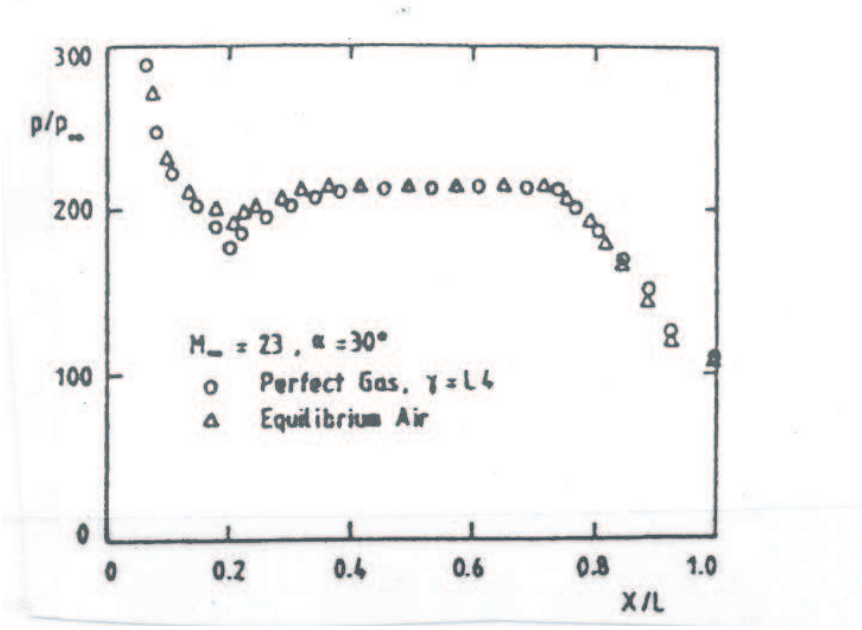

Fig. 1.4 Windward side surface pressure distribution for shuttle for ideal vs. chemically reacting gas.[3]

Plasma Effects: For air at 1 atm pressure, oxygen dissociation begins near 2000 K and is complete at about 4000 K. Nitrogen dissociation begins at about 4000 K and is complete

near 9000 K. At higher post-shock temperatures, ionization becomes important. In a partially ionized flow, the free electrons absorb and reflect electromagnetic radiation, usually in the frequency band of communication systems. In addition, at some level of ionization, the flow will behave quite differently than a weakly-ionized or neutral flow, since the interatomic forces will have a strong electrical interaction component, which will lead to differences in transport properties.

Viscous and Rarefaction Effects: Finally, for very high speeds at low density, which might correspond to a high atmospheric altitude, the mean free path, which is the average distance that a molecule or atom travels between collisions with its neighbors, can be large than a characteristic length of the vehicle. This effect is represented by the Knudsen number λ/L, and we can see from the figure below that when the mean free path is too large, and Kn approaches unity, then the familiar Navier-Stokes equations can no longer be closed. Another approach to modeling the flow must be used. The viscous interaction parameter,

$$\bar{V}'_{\infty} = M_{\infty}\frac{\sqrt{C'_{\infty}}}{\sqrt{Re_{\infty L}}} \quad ,$$

where $C'_{\infty} = (\mu_{\infty}T')/(\mu' T_{\infty})$ is the Chapman-Rubesin viscosity coefficient based on reference temperature conditions. The variation of this parameter for a Shuttle re-entry is shown in Fig. 1.5, and the regimes where an inviscid approach to flow analysis cannot be used are clearly shown. In fact, inviscid analysis can only be used in the "hypersonic" regime, which is characterized by high Reynolds and low Mach number conditions. At higher altitudes, the reverse situation of high Mach and low Reynolds requires careful handling of the viscous interactions that affect the invisid flow.

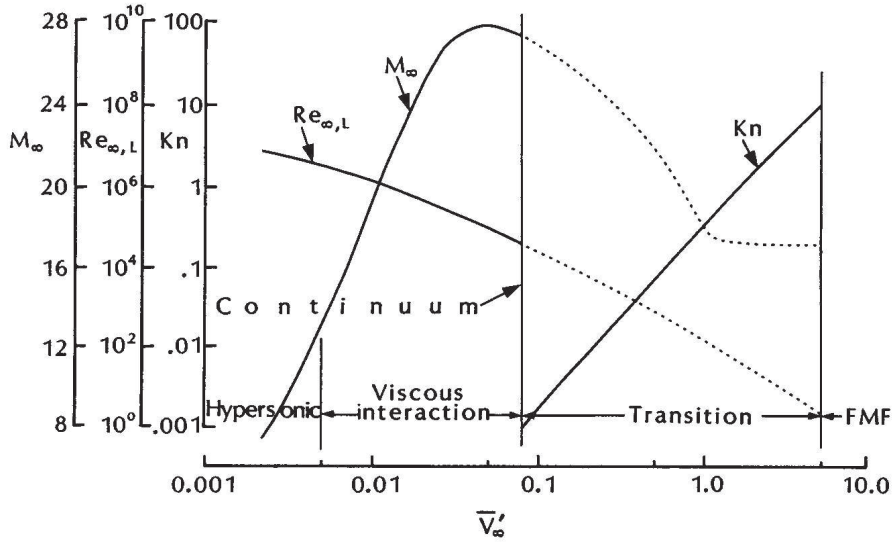

Fig. 1.5 Viscous interaction parameter variation for a Shuttle re-entry. [3]

Trajectory Dependence: As mentioned above, air chemistry is significantly different at the high temperatures encountered in hypersonic flight applications. Vibrational excitation of molecules, dissociation, and ionization will all occur as temperature is increased.

However, with the exception of vibrational excitation, the onset and range of the these effects will also vary with density, or pressure. To illustrate this point, a velocity altitude map is shown in Fig. 1.6. Different trajectories for re-entry, corresponding to different values of the ballistic parameter, m/Ac_L, are shown on the figure (note the range indicated for Shuttle trajectories) . The shaded regions on the map delineate regions of thermal or chemical activity and the edges are sketched to represent where there is 10 % and 90 % excitation or dissociation (assuming local thermodynamic equilibrium or LTE). The temperature values that describe these ranges are those behind the bow shock, and the density behind the bow shock depends on the altitude and the speed. Density also decreases with increasing altitude, and the onset and completion boundaries for each of these effects shifts to a lower temperature. This should be taken as a qualitative indication only; these temperature values are not fixed on a linear scale. Another point to bear in mind is that the area of vibrational excitation corresponds only to the range in which the vibrational modes of the relevant diatomic molecules (O_2, N_2, and NO) become fully excited. Vibrational excitation will be addressed more extensively in following sections, but the important point here is that the undissociated molecules still possess significant vibrational energy, and this in turn is coupled to dissociation.

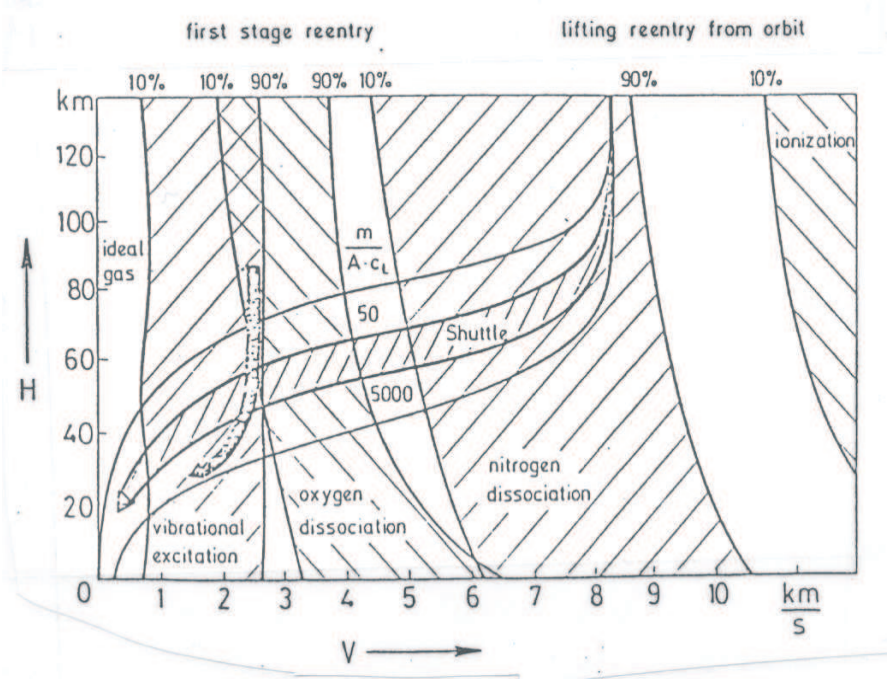

Fig. 1.6 Velocity altitude map for earth re-entry showing different thermochemical regimes.

Nonequilibrium Effects: In addition to these effects, when the characteristic flow time is much shorter than the time to complete chemical reactions or energy exchange mechanisms, then the flow can be in a nonequilibrium state. It is in this aspect that the Damkohler number plays a determining role. Note that for a given situation there can be either thermal nonequilibrium, chemical nonequilibrium, or both. This is a subject of considerable importance, as the interpretation of physical and chemical phenomena in hypersonic flow applications often depend on the assumption of thermal and chemical equilibrium, which allows for a simpler characterization of the thermal and chemical

state of the flow. This assumption is often used without justification, and it is the objective of many present research activities to investigate the limits of this assumption!

Ground Test: It is apparent, even to the casual observer, that hypersonic vehicles are not yet readily available for human transportation. At present, there is only the Space Shuttle, and the lifetime of this vehicle has already been officially fixed (even though it is already operating BEYOND the design lifetime). Consequently, there is very little empirical data on vehicle design and performance and many design parameters have been barely explored. Part of the reason for this is the difficulty in simulating flight conditions on the ground. There relationship between actual flight data and the data from measurements in ground test facilities is not yet well understood. Unfortunately, flight experiments are expensive, and even ground tests in high-enthalpy facilities are not cheap, so there is relatively little data to guide the development of analytical and numerical tools for these applications.

In the following sections, an engineering background for the analysis of hypersonic and high-enthalpy flows is developed. As some of the hypersonic flow regime can be usefully addressed with perfect gas analyses (at least to the limit of the onset of real-gas effects) a review of perfect gas flow analysis is included. Next, exact and analytical representations of caloric imperfection are derived, and the differences between calorically perfect and imperfect gas results are compared for flow through a normal shock. Following this comparison, the concepts underlying chemically reacting flow are introduced in a manner consistent with the statistical mechanical approach taken to address caloric imperfection. Finally, the implications of caloric imperfection and chemical reaction for ground test simulation of hypersonic flows are addressed.

2.Basic Definitions and Thermodynamic Concepts

When chemical and thermal equilibrium (based on the definitions given in the preceding section) conditions are satisfied, then the system is said to be in a state of thermodynamic equilibrium. Classical thermodynamics treats changes between equilibrium states as being characterized by a succession of intermediate equilibrium states that transition infinitely slowly from one to the other. These changes are, of course, reversible. However, in hypersonic flow, many processes irreversible, as for example the passage of flow through a shock wave. An irreversible process is one that takes place through a succession of nonequilibrium states. To understand this, it is assumed that in each intermediate state, the system is in local thermodynamic equilibrium, although not necessarily with its surroundings, and one can then look at the integral of the process. In this way coupled problems of gas dynamics and heat transfer can be treated.

Just as one can distinguish between reversible and irreversible processes, a distinction is also made between perfect and real gases. In the introductory section, a "real" gas was not explicitly defined. For physical chemists, a real gas denotes a situation where the intermolecular forces must be considered in the caloric and thermal description of the gas. This implies that a "real gas" is a thermally imperfect gas, since consideration of the intermolecular forces is more important during phase change for a substance. To illustrate this point, consider the general case of the typical intermolecular interaction potential for neutral molecules, the Van der Waal's, or dispersion interaction. (The

intermolecular force, $F(r)$, is related to the interaction potential, $U(r)$, by $F(r) = -(dU(r)/dr)$.) The dispersion interaction is the most common for atmospheric pressure and room temperature air. The interaction potential for the dispersion forces is sketched in Fig. 2.1. It has two parts, an attractive potential that operates over long distances, but typically falls off at a distance of about 10 diameters, and a repulsive potential that dominates the interaction at short distances, such as between neighboring molecules.

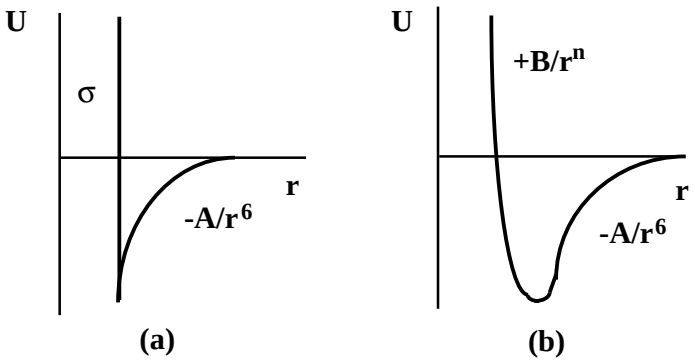

Fig. 2.1. Van der Waals interaction potential (a) and Lennard-Jones interaction potential (b).[8]

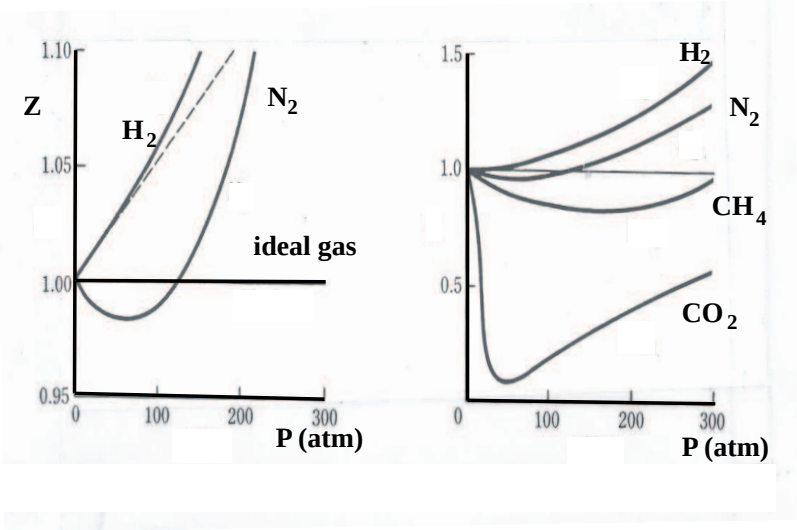

Fig. 2.2. Compressibility of various gases as a function of pressure at $T = 273$ K.[8]

If the average spacing between the molecules is greater than about 10 diameters, then the intermolecular forces can be safely ignored. For air this is a valid assumption to pressures up to 1000 atm and for temperatures above about 30 K. Obviously, when the condensation temperature of any constituent species is approached, the intermolecular forces are important and they play an important role in the phase change. For other species, such as CO_2, the range of validity of the perfect gas assumption is less than for air. This is illustrated in Fig. 2.2, where the compressibility factor Z, which is defined

as

$$Z = v/v_{ideal} = pv/RT \quad ,$$

is shown as a function of pressure at 273 K for a number of pure gases. For a perfect gas $Z = 1$, and we see that for N_2 Z does not differ significantly from unity until very high pressure, but for CO_2 there is considerable variation at modest pressure. Although CO_2 is present in the atmosphere at about 200 ppm, the relatively small concentration does not affect the behaviour of air.

Perfect Gas Equation of State

The perfect gas equation of state is usually presented in terms of moles of a gas and for a single species it is usually written as:

$$pV = \eta R_u T \quad ,$$

where p is the pressure, V is the volume, η is the number of moles, R_u is the universal gas constant, and T is the temperature. There are many more convenient forms of the equation. If we multiply and divide the right hand side of the above equation by the molar mass of the particular species (or mixture, such as air), MW, then perfect gas equation of state becomes

$$pV = (\eta MW)\frac{R_u}{MW}T = MRT \quad ,$$

where M is the mass of the gas species, and R is the specific gas constant for the species or mixture. Dividing the equation by the mass yields,

$$pv = RT \quad ,$$

where the lower case v now denotes the specific volume, which is also the inverse of density, since $v = 1/\rho$. If we substitute this relation, we obtain the more convenient form,

$$p = \rho RT \quad .$$

The density is also equal to the number density of molecules times the mass of an individual molecule, $\rho = nm$. Furthermore, the mass of a molecule is equal to the molar mass of the species divided by the number of molecules in a mole (Avogadro's number), or $m = MW/N_A$. If these two relations are substituted into the perfect gas equation, the following result is obtained,

$$p = n\left(\frac{MWR}{N_A}\right)T \quad .$$

Finally, if we recognize that the combination $MWR = R_u$, then we should also recognize that $R_u/N_A = k$, where k is Boltzmann's constant. This gives us another useful form of the perfect gas equation of state:

$$p = nkT \quad .$$

This equation is also known to physical chemists and engineers as the ideal gas equation of state. Whether it is called perfect or ideal, the meaning remains the same: the description is an approximation of the actual thermal behavior of the gas. For example, according to the perfect gas equation of state, the volume of an ideal gas at constant pressure and 0 K is zero and the volume approaches zero as the pressure is increased to infinity at constant temperature. Both of these scenarios do not consider the possibility of a phase change, which is what actually happens. Still, the equation is reasonably accurate over quite a wide range of property variation. Even when it is not strictly applicable, it can give a useful indication of approximate behavior.

Gas Mixtures: As chemical reactions are often encountered in hypersonic flow applications it is useful to revisit the concepts of mixtures of gases. In the literature about hypersonic and other chemically reacting flows, one finds the components described in terms of:

a. Partial pressure, p_i, where from Dalton's law of partial pressures $\sum_i p_i = p$.
b. Concentrations, C_i, which are the number of moles of species i per unit mixture volume.
c. Mole fractions, χ_i; the number of moles of species i per mole of mixture.
d. Mass fractions, c_i, which is more common in the aerospace community than mole fraction. The mass fraction is the mass of component i per mass of mixture, and it can also be written as $c_i = \rho_i/\rho$.

All of these variables can be related to each other through the equation of state. For example, the mole fraction can be expressed as

$$\chi_i = \frac{\eta_i}{\eta} = \frac{p_i}{p} \quad ,$$

and the mass fraction can be found from the mole fraction as

$$c_i = \left(\frac{MW_i}{MW}\right)\chi_i \quad .$$

By definition, both the mole fractions and mass fractions of a mixture sum to unity, or

$$\sum_i c_i = \sum_i \chi_i = 1 \quad .$$

The gas constant for the mixture R_m can be found from the component values and the mass fractions as

$$R_m = \sum_i c_i R_i \quad ,$$

and the relation between mass fraction of a species and its number density is

$$c_i = \frac{\rho_i}{\rho} = \frac{n_i MW_i}{\rho N_A} \quad ,$$

which is useful for relating spectroscopically measured quantities to results from numerical simulations for hypersonic flow applications.

Real Gas Equation of State

Although most of the discussion concerns thermally perfect gases, it is instructive to look at other equations of state that can be used for non-perfect gas situations. The most well-known of these equations is the Van der Waal's equation,

$$p = \frac{RT}{v-b} - \frac{a}{v^2} \quad .$$

This equation expresses the relationship between the thermodynamic variables in the same way as the perfect gas equation, but with an important modification to account for the attractive forces of real gas behaviour at high density in the second term. Recall that the long-range attractive potential scaling was $\approx -A/R^6$, and note that the second term in the Van der Waal's equation of state above is $-a/v^2$. Clearly, the second term is intended to account for the attractive potential, which becomes important as density increases. This equation provides a useful qualitative picture of real gas behaviour, but it is not quantitative. For example, the onset of the real gas behaviour also depends on temperature, and this effect is not included in the above equation.

Fortunately for most applications involving hypersonic flows of air, the departure from thermal perfection is minimial, as shown in the figure on compressiblity. For CO_2, this is not the case, and as some hypersonic ground test facilities, such as the VKI Longshot Facility use CO_2, it is important to take into account its thermal imperfection when considering the test conditions. As the remaining examples are concerned only with air, thermal imperfection will not be considered further in the following discussions.

3. Thermally and Calorically Perfect Gases - Supersonic Flow

If we revisit for a moment the perfect gas result

$$du = c_v dT \quad ,$$

and the analagous result for c_p,

$$dh = c_p dT \quad ,$$

we see that these two expressions lead to the mathematical definitions of thermally and/or calorically perfect gases for single component systems (or for non-reacting mixtures). For a calorically perfect gas, the specific heats are constant (as is γ), and both expressions can be integrated immediately to yield

$$u = c_v T \quad \text{and} \quad h = c_p T \quad .$$

For lower speed compressible flow, this assumption is usually acceptable and a great deal of analytical results can be obtained for the analysis of supersonic flows. A useful compendium of such results is the NACA Publication 1135 "Charts and Tables for Compressible Flow" [4]. There are many excellent and comprehensive text books that have been written on the subject of compressible flow. Some of the more commonly encountered texts are those of Anderson [1], Leipmann and Roshko [2], Bertin [3], and Shapiro [5]. Although it was shown to be not the best parameter for defining hypersonic

flow, the Mach number is the most important parameter for defining compressible flows, and the basis of the Mach number is the local speed of sound in the medium of interest. The sound speed, a is defined formally as

$$a^2 = \left(\frac{\partial p}{\partial \rho}\right)_S \quad ,$$

which for a perfect gas, is

$$a^2 = \gamma RT \quad .$$

To find how flow and thermodynamic properties depend on the Mach number, it is convenient to start from the first law of thermodynamics for adiabatic flow in its two differential forms

$$de = -pdv \quad \text{and} \quad de = vdp \quad ,$$

recalling that $h = e + pv$. Writing the total differential for both the internal energy and the enthalpy yields

$$de = \left(\frac{\partial e}{\partial v}\right)_T dv + \left(\frac{\partial e}{\partial T}\right)_v dT = -pdv \tag{3.1}$$

and

$$dh = \left(\frac{\partial h}{\partial p}\right)_T dp + \left(\frac{\partial h}{\partial T}\right)_p dT = vdp \quad . \tag{3.2}$$

From the basic definitions of the specific heats,

$$\left(\frac{\partial e}{\partial T}\right)_v = c_v \quad \text{and} \quad \left(\frac{\partial h}{\partial T}\right)_p = c_p \quad ,$$

and these can be inserted into the respective total differential expressions. If Eq. 3.1 is then divided through by dv, and Eq. 3.2 is divided through by dp, then one obtains after rearranging both equations

$$\frac{dT}{dv} = \frac{-1}{c_v}\left(p + \frac{\partial e}{\partial v}\right) \quad (3.3) \quad \text{and} \quad \frac{dT}{dp} = \frac{1}{c_p}\left(v + \frac{\partial h}{\partial p}\right) \tag{3.4}$$

Dividing one of the original expressions of the first law by the other yields a third relationship among the thermodynamic variables

$$\frac{dp}{dv} = -\frac{p}{v}\left(\frac{dh}{de}\right) \quad . \tag{3.5}$$

As the gases are considered to be thermally perfect, the derivative terms in Eqs. 3.3 and 3.4 vanish since

$$de = c_v dT \quad \text{and} \quad dh = c_p dT \quad .$$

Thus, by making use of the equation of state for an ideal gas, on obtains the simplified relations

$$\frac{dT}{dv} = \frac{-p}{c_v} = \frac{-RT}{vc_v} \tag{3.6}$$

and

$$\frac{dT}{dp} = \frac{v}{c_p} = \frac{RT}{pc_p} \tag{3.7}$$

and

$$\frac{dp}{dv} = \frac{-pc_p dT}{vc_v dT} = \frac{-pc_p}{vc_v} \tag{3.8}$$

If the thermodynamic variables are moved to the LHS of these relations, then

$$\frac{v}{T}\frac{dT}{dv} = -\frac{R}{c_v}, \quad \frac{p}{T}\frac{dT}{dp} = \frac{R}{c_p} \quad \text{and} \quad \frac{v}{p}\frac{dp}{dv} = -\frac{c_p}{c_v} \quad .$$

The expressions can be further simplified by recalling that the definition of γ and the relation $R = c_p - c_v$. Substituting these relations and separating the variables yields finally

$$\frac{dv}{v} = -\frac{1}{(\gamma-1)}\frac{dT}{T}, \quad \frac{dp}{p} = \frac{\gamma}{(\gamma-1)}\frac{dT}{T} \quad \text{and} \quad \frac{dp}{p} = -\gamma\frac{dv}{v} \quad .$$

For the special case of calorically perfect gases the specific heat ratio, γ, is constant and the above expressions can be integrated directly. Taking the exponential of the result yields the isentropic relations

$$v = const \cdot T^{-1/\gamma-1} \quad p = const \cdot T^{-\gamma/\gamma-1} \quad p = const \cdot v^{-\gamma} \quad .$$

From the last relation, one also can directly evaluate the definition of sound speed, as

$$a^2 = \left(\frac{\partial p}{\partial \rho}\right)_s = \gamma\rho^{\gamma-1} = \gamma RT \quad ,$$

which strictly can only be applied to perfect gases. The isentropic relations are a convenient means for relating variations in thermodynamic properties to each other, and to other variables of interest.

For steady, inviscid, non-reacting compressible flows in general, the governing flow equations are

Continuity:	$\nabla \cdot \rho\vec{u} = 0$
Momentum:	$\rho\vec{u} \cdot \nabla\vec{u} = -\nabla p$
Energy:	$\rho\vec{u} \cdot \nabla(h+k) = 0 \quad ,$

where $k = u^2/2$ is the kinetic energy. From the energy equation, it is apparent that total enthalpy is constant in the flow, and this relation can be used to write the equality between the stagnation enthalpy (known from initial conditions, typically from a settling chamber where $u = 0$) and the local value, and this can be written as

$$h_0 = h + \frac{u^2}{2} \quad ,$$

or, for calorically perfect gases

$$c_p T_0 = c_p T + \frac{u^2}{2} \implies \frac{\gamma RT_0}{\gamma - 1} = \frac{\gamma RT}{\gamma - 1} + \frac{u^2 a^2}{2a^2} \quad ,$$

which yields

$$\gamma R T_0 = \gamma R T \left(1 + \frac{\gamma - 1}{2} M^2\right) \quad .$$

Solving this expression for the temperature ratio gives

$$\frac{T_\infty}{T_0} = \left(1 + \frac{\gamma - 1}{2} M_\infty^2\right)^{-1} \quad , \tag{3.8}$$

which, when combined with the isentropic relations, gives the variation of the thermodynamic variables as a function of Mach number for an isentropically expanding flow (the subscript ∞ denotes local conditions). For pressure and density the expressions are

$$\frac{p_\infty}{p_0} = \left(1 + \frac{\gamma - 1}{2} M_\infty^2\right)^{-\gamma/\gamma - 1} \tag{3.9}$$

and

$$\frac{\rho_\infty}{\rho_0} = \left(1 + \frac{\gamma - 1}{2} M_\infty^2\right)^{-1/\gamma - 1} \tag{3.10}$$

Using Eqs. 3.8 to 3.10, it is possible to evaluate the local thermodynamic conditions from the stagnation conditions and knowledge of M_∞. Note that for air at STP, $\gamma = 7/5$.

The governing equations for steady, inviscid supersonic flows admit the possibility of discontinuities in the flow, which can exist as either contact discontinuities (also known as slip streams) or shock waves. If we consider one-dimensional steady, inviscid and supersonic flow as sketched in Fig. 3.1, then the 3 governing equations reduce to

$$\frac{d}{dx}(\rho u) = 0$$

$$\rho u \frac{du}{dx} = -\frac{dp}{dx}$$

$$\rho u \frac{d}{dx}(h + k) = 0$$

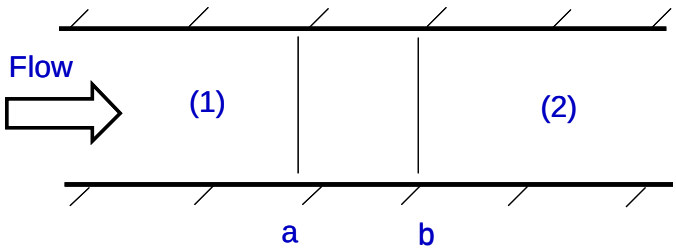

Fig. 3.1. Discontinuous flow region in a supersonic stream.

Referring to Fig. 3.1, the flow in regions (1) and (2) is considered to be uniform, but the properties in these regions are not the same. The two light vertical lines indicate a discontinuous flow region extending from plane a to plane b. Within each of the two uniform flow regions therefore

$$\frac{d}{dx} = 0 \quad ,$$

while within the discontinuous region

$$\frac{d}{dx} \neq 0 \quad .$$

Using definite integrals it is straightforward to evaluate the change in conditions between the two flow regions without knowing the details of the flow properties within the discontinuity. For the continuity equation, this means that

$$\int_a^b \frac{d}{dx}(\rho u)dx = 0 = \rho u]_a^b \Longrightarrow (\rho u)_a = (\rho u)_b \quad \text{or} \quad \rho_1 u_1 = \rho_2 u_2 \quad . \tag{3.11}$$

Since the product ρu is a constant, the momentum equation can be rearranged into a similar, simple definite integral that yields

$$\rho_1 u_1^2 + p_1 = \rho_2 u_2^2 + p_2 \quad , \tag{3.12}$$

and from the energy equation,

$$h_1 + \frac{u_1^2}{2} = h_2 + \frac{u_2^2}{2} \quad . \tag{3.13}$$

Equations 3.11 to 3.13 are known as the Rankine-Hugoniot Jump Relations, and they are used to find the conditions following a normal shock from the upstream values. Although within the shock the flow is both viscous and heat conducting, these effects can be ignored for most practical applications. These equations are applicable to perfect gas wind tunnel flows and to flight (again restricted to conditions where the molecules behave as calorically perfect, which is to a post shock temperature of about 600 to 800 K, depending on the pressure).

For flow through a normal shock, the downstream Mach number (in region 2 of Fig. 3.2 for example)is always subsonic. Normal shock waves are encountered in ground test facilities and in hypersonic flight in the region of the nose and leading edges of the vehicle.

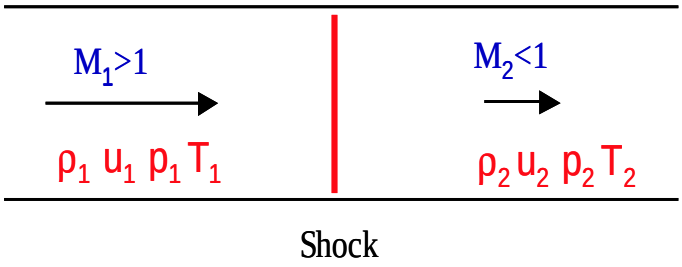

Fig. 3.2. Normal shock in a supersonic stream.

Note that the jump relation for the energy equation can also be written as

$$\frac{\gamma}{\gamma - 1}\frac{p_1}{\rho_1} + \frac{u_1^2}{2} = \frac{\gamma}{\gamma - 1}\frac{p_2}{\rho_2} + \frac{u_2^2}{2} \quad .$$

When this form is used together with the definition of the speed of sound then the change in each variable across the can be written as a function of upstream Mach number and specific heat ratio as

$$\frac{p_2}{p_1} = \frac{2\gamma M_1^2 - (\gamma - 1)}{\gamma + 1} \tag{3.14}$$

$$\frac{\rho_2}{\rho_1} = \frac{(\gamma + 1)M_1^2}{(\gamma - 1)M_1^2 + 2} \tag{3.15}$$

$$\frac{T_2}{T_1} = \frac{[2\gamma M_1^2 - (\gamma - 1)][(\gamma - 1)M_1^2 + 2]}{(\gamma + 1)^2 M_1^2} \quad . \tag{3.16}$$

Expressions based on other parameters can also be developed and a useful compendium can be found in Ref. [naca].

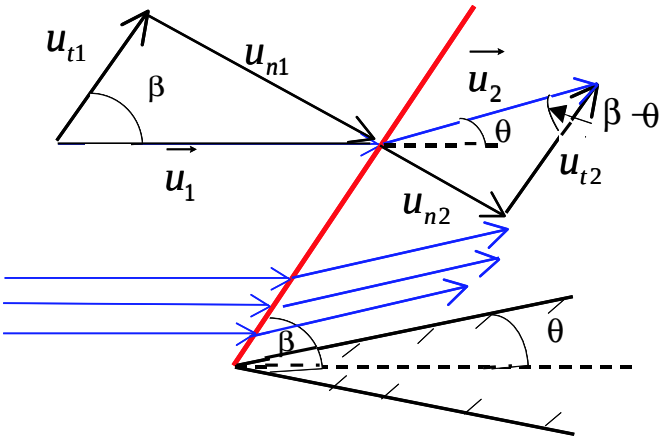

Fig. 3.3. Oblique shock in a supersonic stream.

For supersonic and hypersonic flight applications, oblique shocks are more likely to be found than normal shocks. Oblique shocks arise in the external flow over a body that itself has turned toward the oncoming flow, as happens for example on a deployed flap surface, or on the leading edge of a supersonic wing, as sketched in Fig. 3.3. For an oblique shock flow, it is the velocity component *normal* to the shock that experiences the change. Referring to the Figure then, the oblique shock jump relations are

$$\rho_1 u_{n1} = \rho_2 u_{n2}$$

$$\rho_1 u_{n1}^2 + p_1 = \rho_2 u_{n2}^2 + p_2$$

$$\frac{\gamma}{\gamma - 1}\frac{p_1}{\rho_1} + \frac{u_1^2}{2} = \frac{\gamma}{\gamma - 1}\frac{p_2}{\rho_2} + \frac{u_2^2}{2} \quad ,$$

with the additional constraint that the tangential velocity component is unchanged $u_{t1} = u_{t2}$ (subscripts n and t refer to the normal and tangential components of velocity). Obviously, the energy equation is the same for both normal and oblique shock cases. As with the normal shock relations, all property changes across the oblique shock can be written in terms of the upstream Mach number and the specific heat ratio. The relations are the same as for the normal shock case, except that $M_1 sin\beta$ is used in place

of M_1, where β is the oblique shock angle measured relative to the incoming velocity vector, as indicated in Fig. 3.3. The turning and wave angles are related by

$$\tan(\beta - \theta) = \frac{\tan\beta}{(\rho_2/\rho_1)} \quad .$$

A convenient method for finding flow turning angles is to use the graphical approach wherein the wave angle corresponding to a given turning angle is plotted for different values of the upstream Mach number. A typical representation of this information is shown in Fig. 3.4. For a given Mach number, there are two wave angles that will produce the same deflection angle, corresponding to whether or not the downstream flow is supersonic or subsonic. In addition, a curve is drawn for $\theta = \theta_{max}$, which represents the largest deflection angle for which an oblique shock can stay attached to a body. For a deflection angle $\theta > \theta_{max}$ at a given upstream Mach number, the oblique shock detaches from the body and moves upstream as a detached bow shock.

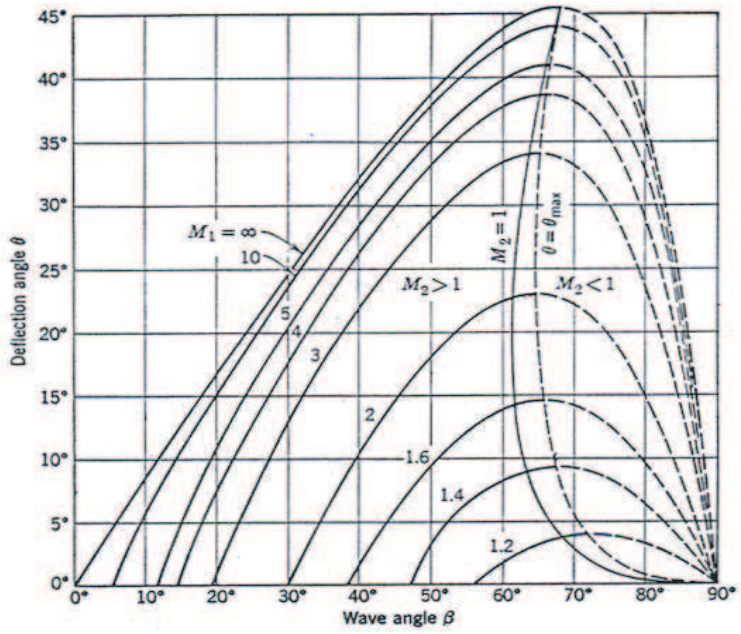

Fig. 3.4. Oblique shock relations for supersonic flow.[2]

In this section, the basic principles of steady, inviscid, supersonic flow have been reviewed. The results that were obtained apply to the flow of perfect gases; that is, gases that are both thermally and calorically perfect. In the next section, the implications of caloric imperfection will be addressed, but it should be noted that the many of the relations that were derived in this section can be extended to conditions where air is calorically imperfect, provided that the variation of specific heat with temperature, for example, is properly accounted for.

4. Thermally Perfect, Calorically Imperfect Gases - Hypersonic Flow

The specific heats for a thermally perfect, but calorically imperfect, gas are functions of temperature only. For this case, the differentials are

$$du = c_v(T)dT \quad \text{and} \quad dh = c_p(T)dT \quad ,$$

and when they are integrated, yield the result that $u = u(T)$ and $h = h(T)$. It is possible to derive both rigorous and simplified analytic expressions for $c_v(T)$ and $c_p(T)$ from statistical mechanics methods. Since the behaviour of gases at high temperatures near a hypersonic vehicle is the primary interest in the present discussion, the case of thermally perfect gases will be explored in greater detail.

The aim of this section is to develop exact and analytical expressions for the temperature dependence of the important thermodynamic properties of thermally perfect, but calorically imperfect gases using the methods of statistical mechanics and quantum mechanics. Owing to the general nature of this Lecture Series, it is not possible to treat this topic in great depth, and only a brief description of the methods and the results is feasible. Concise and clear treatments of these subjects can be found in the books of Vincenti and Krueger [9] and Tien and Lienhard [11], among others. Throughout the following description a number of (simplifying) assumptions are made and, wherever possible, these are discussed in terms of their potential limitations. Again, although the derived results are extremely useful, it should be remembered that they must be applied and interpreted with caution. Following a brief summary of the statistical mechanical approach, which itself is based on quantized energy levels, the quantum mechanical descriptions of particle (atom and/or molecule) energies are discussed. The macroscopic properties are then determined for the cases of atoms, diatomic molecules, and polyatomic molecules.

Statistical Mechanics

Statistical mechanics, like kinetic theory, is focused on the microscopic behaviour of gases; typically at the molecular or atomic level. However, statistical mechanics makes use of statistical methods to avoid having to evaluate every collisional interaction in order to derive macroscopic, equilibrium thermodynamic (actually *thermostatic*) properties. Thermodynamics and statistical mechanics are formally related by the equation

$$S = k \ln \Omega \quad ,$$

which relates the macroscopic property, entropy, to a statistical measure of the randomness of a system, represented by Ω. Specifically, Ω is a measure of how many different ways a collection of microscopic particles can be arranged given the macroscopic conditions and the nature of the particles.

The approach assumes a large collection of particles, such as atoms or molecules, and a macroscopic state is considered to be specified when the number of particles, N, their volume, V, and their energy, E are known. To specify the energy states of the individual particles, the concept of quantized, or discrete, energy levels is used. In general, these states will be at different energies, ϵ_j, although some states can have the same energy, and these are called *degenerate* levels. A key assumption is that the particles are weakly interacting (as for a thermally perfect gas) and that each particle is generally unaffected by the state of any other. Of course, the change from one level to another usually involves some process, such as a bi-particle collision.

Owing to the Heisenberg uncertainty relation, our ability to precisely specify all aspects of the system of particles is limited. The uncertainty relation can be expressed as

$$|\Delta z||\Delta p| \cong h \quad ,$$

where $|\Delta z|$ is the uncertainty in the position of the particle and $|\Delta p|$ is the uncertainty in the particle momentum, and h is Planck's constant. Stated simply, this relation expresses the impossibility of precisely defining both the position and the momentum of a particle at the same time. The relation applies equally to other similarly reciprocal variables (such as energy and time), and a consequence of the relation is that it is not possible to specify a position beyond a certain level of *probability* that the particle will actually be there. In quantum mechanics, this probability is expressed in terms of a wave function, Ψ, and it is governed by the Schrödinger wave equation, which has the following time-independent form,

$$\frac{h^2}{8\pi^2 m}\left(\frac{\partial^2\Psi}{\partial x_1^2}+\frac{\partial^2\Psi}{\partial x_2^2}+\frac{\partial^2\Psi}{\partial x_3^2}\right)+(\epsilon-\epsilon_p)\Psi=0 \quad .$$

In this expression, ϵ is the total energy of the particle, and ϵ_p is the potential energy. The wave function is also normalized such that

$$\int |\psi|^2 dV_x = 1 \quad ,$$

which means simply that the particle must exist somewhere within the system.

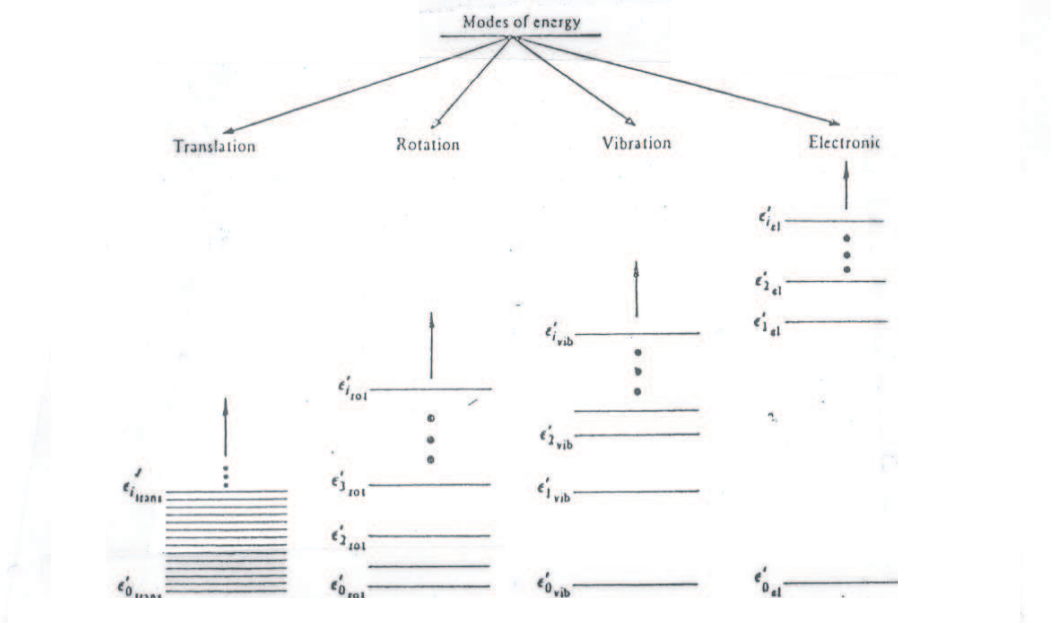

Fig. 4.1. Qualitative picture of the relative energy level spacings for energy modes of molecules.

The quantized energy levels that are populated by the microscopic particles can be separated into *translational* energy and *internal* energy modes. All particles, atoms, molecules, and electrons, possess translational energy, except at temperatures above 0 K. All particles also have internal energy, although for atoms this energy mode is only electronic energy. Molecules can have additional internal energy in the form of rotation and vibration. Thus the total energy of an atomic particle is

$$\epsilon = \epsilon_{trans} + \epsilon_{elect} \quad ,$$

and the total energy of a molecule is

$$\epsilon = \epsilon_{trans} + \epsilon_{elect} + \epsilon_{vib} + \epsilon_{rot} \quad .$$

The spacings of these energy levels are not the same, and the relative magnitude of the difference in energy level spacing for these modes is shown in Fig. 4.1. Within each of the electronic states, there are multiple (bound) vibrational levels, and within each vibrational level, there are multiple rotational levels. In general, the energy level spacings are not constant. Although the translational energy is drawn with discrete levels, these levels are practically indistinguishable at normal flight and test conditions.

At room temperature for a system in equilibrium, all of the atoms and molecules will be in their ground electronic state (that state having zero potential energy). For most of the levels, there are several different states that are possible for the molecule or the atom. For the molecule, these different states may refer to a different orientation of the axis of rotation, which can have three orthogonal directions, but each will have the same energy. So, in general, many of the energy levels shown on the figure are actually degenerate. Thus, for the energy levels $(\epsilon_0, \epsilon_1, ...\epsilon_j)$ there are associated degeneracies $(g_0, g_1, ...g_j)$ that characterize the number of possible states associated with that level and each level has a population of atoms or molecules $(N_0, N_1, ...N_j)$. In general, we consider for any system a collection of groups of energy states. The number of particle in the jth level is N_j and the microstates are C_j and the energy of this level is ϵ_j. For a given macrostate, the number of microstates is W, and the total number of macrostates for a given total system energy and number of particles is

$$\Omega = \sum_j W(N_j) \cong W_{max} \quad .$$

The term, Ω, is a measure of the system disorder, which is also a thermodynamic probability. We are anticipating what we will find by supposing *a priori* that there is one term, W_{max} that contributes the most to Ω.

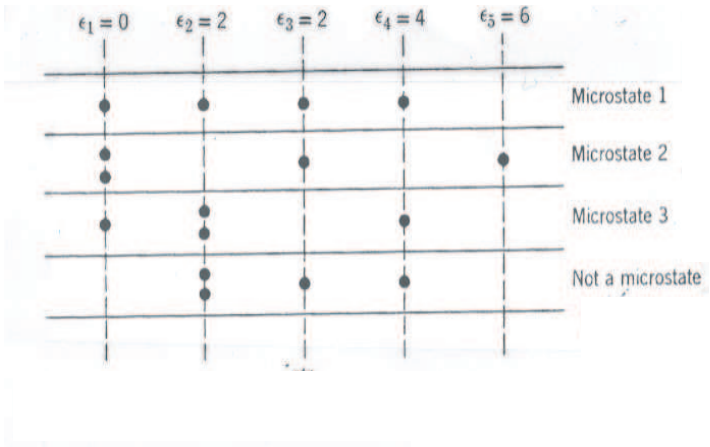

Fig. 4.5. Distribution of population in a simple energy level system.

A simple example of a possible population distribution is shown in Fig. 4.5. The level energies are at the top, and the particles are distributed among these energies. The total energy is the sum for all particles in the row. Three possible population distributions that satisfy the macroscopic constraints of a fixed total number of particles and a fixed total energy are shown. The statistical mechanical approach is based on determining a method for enumerating the possible microstates in such a way as to find the most probable distribution.

One of the key points of the analysis is that the possible number of microstates C_j is greater than the number of particles N_j. Then, the approach is to maximize the expression for $\ln W$ (from looking for a maximum considering that the derivative with respect to the small changes in the number of particles will be equal to zero) subject to the constraints of known total particle number and known system energy using the method of Lagrange multipliers. to find the result. With the assumption that the there is one leading contribution to $\ln \Omega = \ln W_{max}$, we find

$$\ln \Omega = N \left(\ln \frac{\sum_j C_j e^{-\beta \epsilon_j}}{N} + 1 \right) + \beta E \quad .$$

This equation provides the total number of microstates that is consistent with the system constraints of total particles and total energy, but β is an as yet undetermined constant.

For convenience it is useful to define a partition function,

$$Q = \sum_j C_j e^{-\beta \epsilon_j} \quad ,$$

and it is now possible to recognize the leading term in the expression for $\ln \Omega$ as a form of the Boltzmann distribution. This can now be written in a more suitable form,

$$\frac{N_j^*}{N} = \frac{C_j e^{-\beta \epsilon_j}}{Q} \quad .$$

The remaining constant β must be determined using the system constraint of the total energy, but for now there is not enough information to do this. Note that in general the partition function depends on the thermodynamic variables, or $Q = Q(V, T)$.

Up to this point, the classification of the j groupings has been arbitrary. Now it is useful to specify the i energy levels of the system as defining the different groups. With this specification, the Boltzmann distribution becomes

$$\frac{N_i^*}{N} = \frac{g_i e^{-\beta \epsilon_i}}{Q} \quad .$$

This effectively replaces the C_j number of microstates (all having the same energy ϵ_j) with the degeneracy of the particular energy level. Now it is possible to write the relation between the derived result and the system entropy as,

$$S = k \ln \Omega = k \left[N(\ln \frac{Q}{N} + 1) + \beta E \right] \quad .$$

It is possible to use Gibb's relation to evaluate the constant β, since

$$\left(\frac{\partial S}{\partial E}\right)_{V,N} = \frac{1}{T} \quad .$$

Taking the derivative above with respect to the energy, it is clear that $\beta = 1/kT$. Finally, the relationship between the system entropy and the microscopic distribution of particles is

$$S = Nk(\ln \frac{Q}{N} + 1) + \frac{E}{T} \quad ,$$

and this is the fundamental relation between the macroscopic system properties and the microscopic distribution of the particles. From this relation other macroscopic thermodynamic variables can be determined as a function of the microscopic distribution. For example, the total energy is

$$E = \sum_j N_j^* \epsilon_j = \sum_j \epsilon_j \frac{N g_j e^{-\epsilon_j/kT}}{Q} = \frac{N}{Q} \sum_j \epsilon_j g_j e^{-\epsilon_j/kT} \quad .$$

Recall that $Q = Q(V,T)$ and from its definition, it can be differentiated with respect to temperature at constant volume, which yields

$$\left(\frac{\partial Q}{\partial T}\right)_V = \frac{1}{kT^2} \sum_j \epsilon_j g_j e^{-\epsilon_j/kT} \quad .$$

This can be substituted into the expression for the total energy to yield,

$$E = \frac{N}{Q} kT^2 \left(\frac{\partial Q}{\partial T}\right)_V = NkT^2 \left(\frac{\partial (\ln Q)}{\partial T}\right)_V \quad ,$$

where the second form is more convenient. The specific energy is $e = E/M$, where M is the system total mass. For the specific energy, the simplified relation is

$$e = RT^2 \left(\frac{\partial \ln Q}{\partial T}\right)_V \quad , \tag{4.1}$$

and for the specific enthalpy, we obtain a similar form,

$$h = RT + RT^2 \left(\frac{\partial \ln Q}{\partial T}\right)_V \quad .$$

Recall that since

$$c_v = \left(\frac{\partial e}{\partial T}\right)_v \quad \text{and} \quad c_p = \left(\frac{\partial h}{\partial T}\right)_p \quad ,$$

these can also be related to the partition functions. Finally, a relation for pressure that is derived from the Helmholtz potential can also be written as

$$p = MRT \left(\frac{\partial \ln Q}{\partial V}\right)_T = nKT \left(\frac{\partial \ln Q}{\partial v}\right)_T \quad .$$

These relations are most useful for evaluating the thermodynamic properties that are important in hypersonic flow applications. All thermodynamic properties of a collection of particles, atoms or molecules, can be related to the microscopic description of how particles are distributed among the particular species energy levels.

Quantum Mechanics

Once this most probable distribution is found, the populations of the different energy levels are known, and the partition functions can be evaluated. From the partition functions, it is possible to determine the macroscopic thermodynamic parameters. This is a truly general result, for LTE conditions; however, the details of how these populations are arranged among the energy levels depend on quantum mechanical considerations of the energy level spacings for a given system. To find how energy levels are distributed, the Schrödinger equation is solved separately for the energy of interest. As this is of interest to many fields, one can simply look for the four exact solutions to the time-independent Schrödinger equation:

1. Particle in a box ⇒ translational energy
2. Rigid rotor ⇒ rotational energy
3. Harmonic oscillator ⇒ vibrational energy
4. Single electron in a central field ⇒ electronic energy

Again, owing to the constraints of this Lecture Series, it is not possible to go through all the details of these solutions (see [9-11]). Instead, the simplest case of translational energy will be presented and then combined with the results of the other solutions.

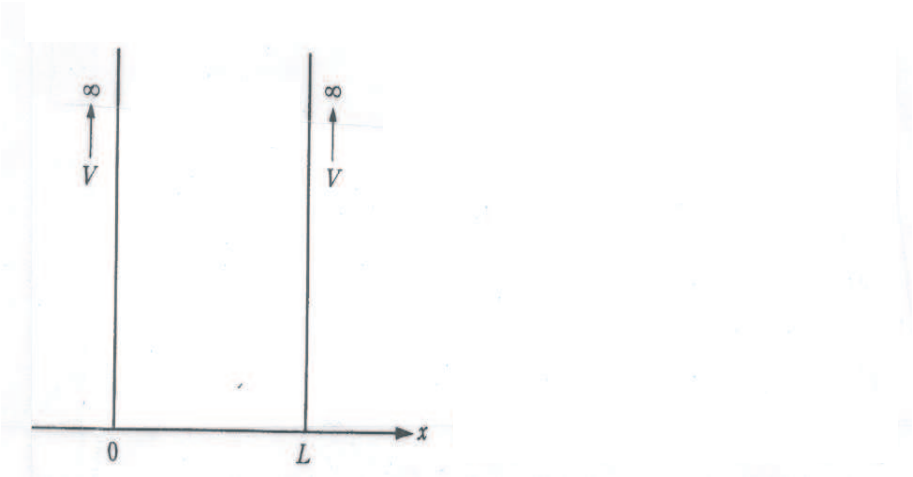

Fig 4.6. Idealized representation of a particle in a box.

Particle in a Box

The case of the particle in a box is the simplest representation of translational energy quantizaton. A box is constructed as shown below in Fig. 4.6, which illustrates only one dimension of the box. There are two walls on the x-axis, at $x = 0$ and $x = a$. Inside the box the potential energy is zero ($V = 0$), but at the walls the potential energy is

infinite ($V = \infty$) and this gives an infinite strength repulsive force at the wall to confine the particle within the box. Outside the box, the potential energy is also infinite. The time independent wave equation for the whole system is

$$\nabla^2\Psi + \frac{8\pi^2 m}{h^2}(\epsilon - \epsilon_p)\Psi = 0 \quad .$$

Owing to the boundary condition, it is clear that $\Psi = 0$ at $x = 0, a$ and that outside of the box, $\Psi = 0$ also, meaning that the particle has no probability of being outside the box. Within the box, where the potential energy is zero, the wave equation takes the form

$$\nabla^2\Psi + \frac{8\pi^2 m}{h^2}(\epsilon)\Psi = 0 \quad .$$

The boundary conditions are the same in each of the three coordinate directions, and this gives a second order differential equation in x, y, z, which can be solved by separation of variables,

$$\Psi(x, y, z) = X(x)Y(y)Z(z) \quad .$$

Following substitution, this gives

$$\frac{1}{X}\frac{d^2X}{dx^2} + \frac{1}{Y}\frac{d^2Y}{dy^2} + \frac{1}{Z}\frac{d^2Z}{dz^2} + \frac{8\pi^2 m}{h^2}\epsilon = 0 \quad .$$

Because the sum of these pure derivatives is equal to a constant, this constant can be set as $k_x = (8\pi^2 m/h^2)\epsilon_x$, etc. Doing this yields three ordinary differential equations of the form

$$\frac{d^2X}{dx^2} + \frac{8\pi^2 m}{h^2}\epsilon_x X = 0 \quad ; X(0) = X(a) = 0 \quad .$$

The general solution to an equation of this type is

$$X = A_x \sin\left(\sqrt{\frac{8\pi^2 m\epsilon_x}{h^2}}x\right) + B_x \cos\left(\sqrt{\frac{8\pi^2 m\epsilon_x}{h^2}}x\right) \quad .$$

Imposing the boundary conditions yields $B_x = 0$ and $\sqrt{8\pi^2 m\epsilon_x/h^2} = n_x\pi/a$, where $n_x = 1, 2, 3, ...$ The solution for X is then

$$X = A_{nx} \sin\left(\frac{n_x}{a}\pi x\right) \quad \text{where} \quad n_x^2 = \frac{8a^2 m\epsilon_x}{h^2} \quad .$$

For all three directions then, the quantized energy components in each direction are

$$\epsilon_{x_i} = \frac{n_{x_i}^2 h^2}{8ma_i^2} \quad ,$$

where the i values represent the directions x, y, z and the n_{x_i} are the quantum numbers. The total translational energy of the particle in the box is therefore

$$\epsilon_{tr} = \frac{h^2}{8m}\left(\frac{n_x^2}{a^2} + \frac{n_y^2}{b^2} + \frac{n_z^2}{c^2}\right)$$

The wave function has the form

$$\Psi_{n_x,n_y,n_z} = A_{nx} \sin \frac{n_x \pi x}{a} A_{ny} \sin \frac{n_y \pi y}{b} A_{nz} \sin \frac{n_z \pi z}{c} \quad ,$$

and by making use of the normalization property, $\int \Psi^* \Psi dV = 1$, of the wave function, it is possible to evaluate the remaining constants. Doing this involves integrating the wave function times its complex conjugate over the confines of the box,

$$\int \Psi^* \Psi dV = (A_{nx} A_{ny} A_{nz})^2 \int_0^a \sin^2 \frac{n_x \pi x}{a} dx \int_0^b \sin^2 \frac{n_y \pi y}{b} dy \int_0^c \sin^2 \frac{n_z \pi z}{c} dz \quad .$$

This produces the relatively simple result that $(A_{nx} A_{ny} A_{nz}) = \sqrt{8/abc}$. Finally, we have the result for the wave function for translational energy

$$\Psi_{n_x,n_y,n_z} = \sqrt{\frac{8}{abc}} \sin \frac{n_x \pi x}{a} \sin \frac{n_y \pi y}{b} \sin \frac{n_z \pi z}{c} \quad .$$

Note that for a single dimension, which is a little easier to keep up with in typing, the result for probability is

$$\Psi(x) = \sqrt{2/a} \sin \frac{n \pi x}{a} \quad ,$$

the translational energy is $\epsilon = n^2 h^2 / 8ma^2$, and the quantum numbers are $n = 1, 2, 3, ...$ It is apparent that the energy is increasing as the square of the quantum number, so the energy spacing is increasing at higher levels.

The separation between energy levels is

$$\Delta\epsilon = \epsilon_{n+1} - \epsilon_n = \frac{(2n+1)h^2}{8ma^2} \quad ,$$

which is only important for a very small box. For larger containers that represent practical length scales, the energy differences become immeasurably small ($\sim h^2/ma^2$). Considering nitrogen, the mass of a molecule is .028 kg/mol /$6(10)^{23}$molecules/mol, or $4.7(10)^{-26}$kg/molecule and the spacing is $\sim 1.2(10)^{-42}$J/a^2. For dimensions of systems of particles that are of interest in hypersonics, ($> 10^{-6}$m) the spacing between energy levels will be quite small.

The general case we have examined considers a box of arbitrary dimensions. We can look at the special case of cube and use the result to illustrate the concept of degeneracy. For this case, the total energy is

$$\epsilon = \frac{h^2}{8mL^2}(n_x^2 + n_y^2 + n_z^2) \quad ,$$

since the sides are $a = b = c = L$. The wave function of the lowest energy level is $\Psi_{1,1,1}$ and this level has a total translational energy of $\epsilon_1 = 3h^2/8mL^2$. The next level occurs for a quantum number change of 1, and there are three possible wave functions for this level, $\Psi_{2,1,1}, \Psi_{1,2,1}$, and $\Psi_{1,1,2}$. Each of these wave functions corresponds to a

distinct and separate state, but all have the same energy, $\epsilon_2 = 6h^2/8mL^2 = 2E_1$. These levels are said to be degenerate. The assumption of a cubic box is responsible for the degeneracy. If the box has sides of arbitrary length, the symmetry in the system is removed, as is the degeneracy.

Rigid Rotor

To understand the quantum mechanical evaluation of the rotational energy of molecules, it is best to consider the example of a rigid rotor for a diatom. This is illustrated below in Fig. 4.7, which shows a diatom as two nuclei connected by a rigid bar. The spacing between the two nuclei is the equilibrium interatomic separation R_e, which corresponds to the zero energy point of vibration for a harmonic oscillator. To solve for the rotational energy distribution it is convenient to ignore the fact that the vibrational and rotational energies are actually coupled and that there is centrifugal distortion of the molecule at high rotational energy.

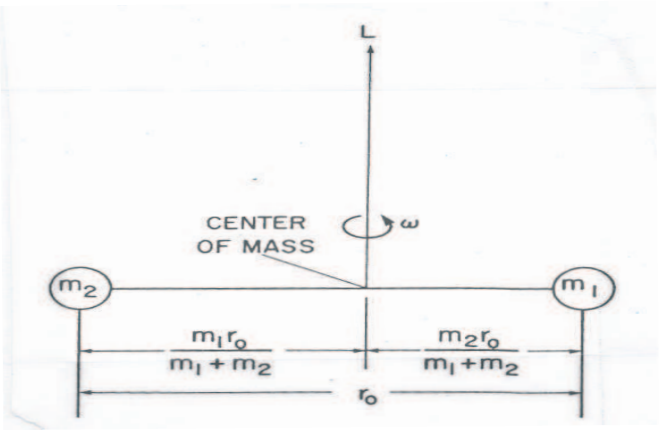

Fig 4.7. Idealized representation of a rigid rotor.

Normally, it is easiest to solve for the rotational energy in a spherical coordinate system and then use variable substitution to find the expression for the rotational energy,

$$\epsilon_{rot} = J(J+1)\frac{h^2}{8\pi^2 I} \quad ,$$

where the moment of inertia of the diatom $I = \mu R_e^2$ and J is the rotational quantum number. As J increases, the rotational energy increases as the square of J. Each value of E_{rot} is degenerate, meaning that there are multiple levels of the same rotational energy, and the value of the degeneracy is equal to $g_r = 2J + 1$ (this came from a constraint of the solution for the rotator). In spectroscopy, the rotational constant for diatomics is written as $B = \frac{h^2}{8\pi^2 I}$. This yields the expression for rotational energy that is most commonly encountered in physical chemistry and in hypersonics,

$$\epsilon_{rot} = BJ(J+1) \quad ; J = 0, 1, 2, ... \quad .$$

Harmonic Oscillator

The simplest representation of the vibrational motion is that of a harmonic oscillator. A conceptual rendering of this system is shown in Fig. 4.8. The two nuclei are considered to

be attached by a spring, with constant k, and equilibrium spacing R_e. The problem can be considered as a reduced mass attached to a fixed wall by a spring with a coordinate system $x = R - R_e$. The potential energy of the spring is $V = kx^2/2$. Again, from the solution of the appropriate wave equation description of the system, the allowed (quantized) values of the vibrational energies are

$$\epsilon_{vib} = \frac{h}{2\pi}\omega(v + \frac{1}{2}) \quad ; \quad v = 0, 1, 2, 3, ... \quad ,$$

where v is the vibrational quantum number and ω is the characteristic vibrational frequency (which has the classical value $\sqrt{k/\mu}$ for the idealized oscillator). Note that even at $v = 0$, there is still vibrational energy $= h\nu/2$, and this is called the zero point energy of the system. Also, for the harmonic oscillator the energy levels are equally spaced, and the degeneracy of each level is unity. For polyatomic molecules there are usually more vibrational modes, and these can be degenerate if the symmetry of the molecule allows it. However, for some polyatomics, such as for CO_2, the vibrational modes can be considered to be independent, and each one can be quantized separately and summed to obtain the total vibrational energy.

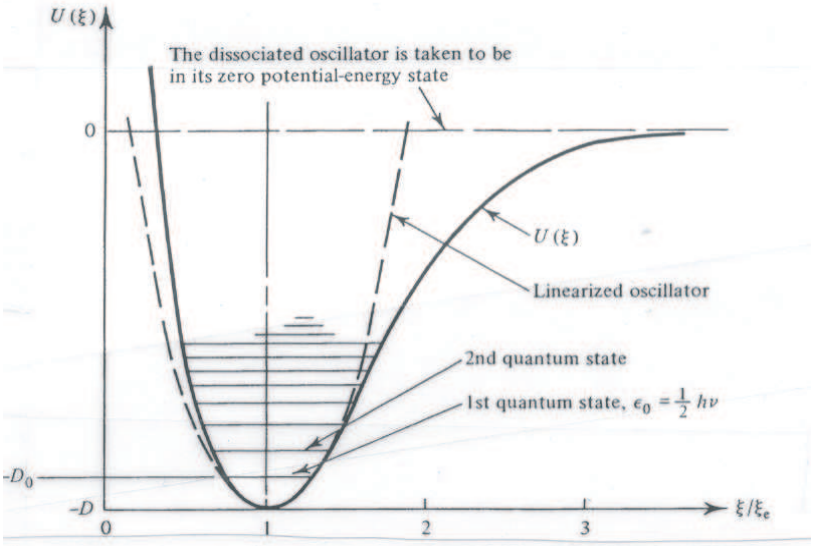

Fig 4.8. Idealized representation of a harmonic oscillator compared to actual diatom.

Corrections to Simple Model

In reality, diatomic molecules are not harmonically oscillating rigid rotors and each energy mode interferes with the other. For example, when the vibrational energy is very large, the spring restoring force becomes non-linear and the potential energy is no longer parabolic. This is shown in the figure of the potential energy diagram for a diatomic molecule. To account for this effect accurately, more terms are used in the vibrational energy, such as

$$\epsilon_{vib} = h\nu \left[(v + \frac{1}{2}) - x_e(v + \frac{1}{2})^2 \right] \quad .$$

With the additional term, the vibrational spacing is no longer constant, but decreases with increasing v.

There is also a vibration-rotation interaction that follows the anharmonicity. Since the internuclear spacing increases for the higher v levels, the moment of inertia increases also, and so the rotational energy must also be corrected. This is also done using a term to correct the rotational constant that is dependent on the vibrational quantum number,

$$\epsilon_{rot} = B_v J(J+1) = (B - \alpha_e(v + \frac{1}{2}))J(J+1) \quad .$$

These correction factors are usually determined from small perturbation theory and they are applied to the general solution of the idealized system for each of the energy modes.

Partition Functions and Thermodynamic Quantities

Instead of a single particle in a box, we now consider the case of multiple particles that only weakly interact within a box. To evaluate the partition function for the translational energy for this situation, recall that the expression for the translational energy for the particle in a box was

$$\epsilon_{tr} = \frac{h^2}{8m}\left[\left(\frac{n_x}{a}\right)^2 + \left(\frac{n_y}{b}\right)^2 + \left(\frac{n_z}{c}\right)^2\right] \quad ; \quad n_x, n_y, n_z = 1, 2, 3, \ldots \quad .$$

The partition function represents the sum of all of the energy levels, and for the translational energy this means

$$Q = \sum_i e^{-\epsilon_{tri}/kT} = \sum_{n_x=1}^{\infty} \exp\left(\frac{-n_x^2 h^2}{8mkTa^2}\right) \sum_{n_y=1}^{\infty} \exp\left(\frac{-n_y^2 h^2}{8mkTb^2}\right) \sum_{n_z=1}^{\infty} \exp\left(\frac{-n_z^2 h^2}{8mkTc^2}\right) \quad .$$

This expression can be evaluated by noting that

$$\sum_{n_x=1}^{\infty} \exp\left(\frac{-n_x^2 h^2}{8mkTa^2}\right) \cong \int_0^{\infty} \exp\left(\frac{-n_x^2 h^2}{8mkTa^2}\right) dn_x = a\sqrt{\frac{2\pi mkT}{h^2}} \quad .$$

Folowing a similar treatment of the other quantum numbers and noting that $(abc = V)$ one obtains

$$Q_{tr} = V\left(\frac{2\pi mkT}{h^2}\right)^{3/2} \quad .$$

As we anticipated, the $Q_{tr} = Q_{tr}(V, T)$. Again, the assumptions in this derivation were that $T > 5$ K, and weakly interacting particles. With the partition function known, the translational specific energy can be evaluated by using Eq. (10-1) as

$$e_{tr} = RT^2\left(\frac{\partial \ln Q_{tr}}{\partial T}\right)_v = RT^2\frac{3}{2T} = \frac{3}{2}RT \quad .$$

The contribution to the specific heat at constant volume from the translational energy is then

$$c_{vtr} = \frac{3}{2}R \quad .$$

This component of the specific heat is the same for atoms and molecules. Additional contributions come from internal energies, of which the electrical energy contributes to both atoms and molecules, while only molecules have rotational and vibrational energy modes.

For molecules, the partition function would normally be determined by summing all of the energy levels for these modes as

$$Q = \sum_i g_i e^{-\epsilon_i/kT} = \sum_i g_i e^{-(\epsilon_{tri}+\epsilon_{roti}+\epsilon_{vibi}+\epsilon_{electi})/kT} \quad .$$

However, to simplify the evaluation we once again assume that all the energy modes are independent and then we factor the sums

$$Q = \sum_i g_{tr_i} e^{-\epsilon_{tri}/kT} \sum_i g_{r_i} e^{-\epsilon_{roti}/kT} \sum_i g_{v_i} e^{-\epsilon_{vibi}/kT} \sum_i g_{el_i} e^{-\epsilon_{electi}/kT} = Q_{tr} Q_{rot} Q_{vib} Q_{elect} \quad .$$

This very important simplifying assumption allows us to write the energy as

$$e = RT^2 \left(\frac{\partial \ln Q_{tr}}{\partial T} \right)_v + RT^2 \sum_{int} \left(\frac{\partial \ln Q_{int}}{\partial T} \right)_v = e_{tr} + \sum_{int} e_{int} \quad ,$$

which also simplifies the expression for the specific heat,

$$c_v = \left(\frac{\partial e}{\partial T} \right)_v = c_{vtr} + \sum_{int} c_{vint} \quad ,$$

and for the pressure

$$p = MRT \left[\left(\frac{\partial \ln Q_{tr}}{\partial V} \right)_T + \left(\frac{\partial \ln Q_{int}}{\partial V} \right)_T \right] \quad .$$

For the electronic mode, which contributes for both atoms and molecules, the energy level spacings are typically very large. Because of this, there is no closed form analytical expression for the electrical partition function. Rather, it is evaluated by summing the levels, and usually only the lowest levels must be considered. The electrical states of atoms and molecules are often degenerate, so some care should be taken in the evaluation. If we define a characteristic electronic temperature as $\Theta_i^e = \epsilon_{electi}/k$, we can write

$$Q_{elect} = g_0 + g_1 e^{-\Theta_1^e/T} + g_2 e^{-\Theta_2^e/T} + \ldots \quad .$$

By convention, the electronic energy of the zeroth state is taken as zero. Generally two terms are enough for most cases, and the error for neglecting the next term is very small. (Beware of an important exception to this: atomic oxygen which has a triplet, nondegenerate ground state!) The electrical contribution to the specific energy is then

$$e = R\Theta_1^e \frac{(g_1/g_0) e^{-\Theta_1^e/T}}{1 + (g_1/g_0) e^{-\Theta_1^e/T}} \quad .$$

The quantized rotational energy that was determined from the solution of the wave equation for a rigid rotor was $\epsilon_{rot} = BJ(J+1)$ and the degeneracy was $2J+1$ for the different J levels. If we define a characteristic rotational temperature as $\theta_r = B/k$, then we can evaluate the rotational partition function as

$$Q_{rot} = \sum_J (2J+1) e^{-J(J+1)\theta_r/T} \quad .$$

For most applications, the temperature will be much greater than the characteristic rotational temperature, which is usually on the order of 1 to 5 K. (Beware of the exception: molecular hydrogen, which has $\theta_r = 85$ K.) We can therefore argue that for $\theta_r/T << 1$ the summation is approximately equal to the area under the curve of the "continuous" function, or

$$Q_{rot} = \int_0^\infty (2J+1) e^{-J(J+1)\theta_r/T} dJ \quad .$$

This can be evaluated easily by the substitution $z = J(J+1)$ as

$$\int_o^\infty e^{-z\theta_r/T} dz = \frac{T}{\theta_r} \quad .$$

For diatomic molecules, the result also depends on whether or not the two nuclei are different, with

$$Q_{rot} = \frac{T}{\sigma\theta_r} \quad ,$$

and $\sigma = 2$ for homonuclear molecules and $\sigma = 1$ for heteronuclear molecules. For either type of diatom, the same values of $e_{rot} = RT$ and $c_{rot} = R$ are obtained for the rotational contributions to the specific energy and specific heat at constant volume. The Boltzmann distribution of molecules among the rotational energy levels is then

$$\frac{N_J}{N} = \frac{(2J+1)\sigma\theta_r}{T} e^{-J(J+1)\theta_r/T} \quad .$$

For a diatomic molecule, the rotational mode becomes fully excited at very low temperatures, and it contributes a constant value to the specific heat at higher temperature values.

The solution to the Schrödinger wave equation for a harmonic oscillator gave a quantized vibrational level energy of $\epsilon_{vibv} = h\nu(v + 1/2)$. For convenience, it is easiest to look at the distribution relative to the zero point energy, and we will evaluate the vibrational partition function as

$$Q_{vib} = \sum_v e^{-vh\nu/kT} \quad .$$

As in the other examples, we define a characteristic vibrational temperature as $\theta_v = h\nu/k$ and we then have

$$Q_{vib} = \sum_v e^{-v\theta_v/T} = \sum_v x^v = \frac{1}{(1-x)} \quad \text{where} \quad x = e^{\theta_v/T} \quad .$$

The evaluation of this summation in this way requires that $x < 1$, but of course the expression is used beyond this range. We then find that the vibrational partition function is

$$Q_{vib} = \frac{1}{1 - e^{-\theta_v/T}} \quad .$$

The contribution of the vibrational energy to the specific energy is

$$e_{vib} = RT \frac{\theta_v/T}{e^{\theta_v/T} - 1} \quad ,$$

and the contribution of the vibrational mode to the specific heat at constant volume is

$$c_{vvib} = R \left[\frac{\theta_v/2T}{\sinh(\theta_v/2T)} \right]^2 \quad .$$

The characteristic vibrational temperatures are on the order of 2200 K for O_2 and 3390 K for N_2. In contrast to the rotational mode, the vibrational contribution is not full at temperatures of interest in hypersonics. Thus, the vibrational contribution will change with temperature, and this has significant impact on the analysis of high temperature flows.

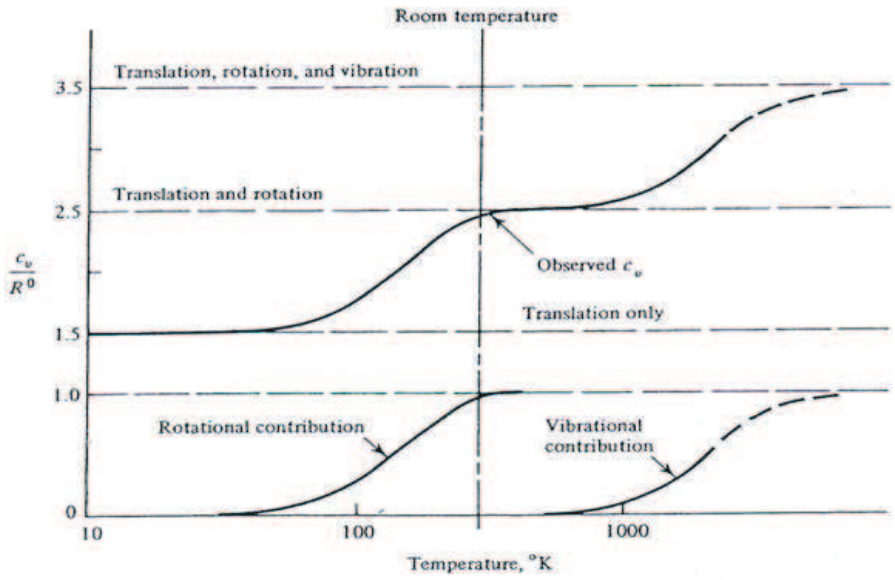

Fig 4.9. Specific heat at constant volume as a function of temperature for H_2 showing the different contributions.[16]

Finally, we can obtain a useful result for the specific heat at constant volume of a diatomic molecule by combining the results of the previous examples

$$\frac{c_v}{R} = \frac{5}{2} + \left[\frac{\theta_v/2T}{\sinh(\theta_v/2T)} \right]^2 \quad .$$

This result is plotted in Fig. 4.9, as a function of temperature for H_2. We see that the vibrational mode contributes roughly $R/2$ when $T/\theta_v = .33$. This also means that the

specific heat ratio γ, which has the value $(7/2)/(5/2) = (7/5)$ at room temperature, decreases to $9/7$ when the vibrational mode is fully excited.

Another important attribute of the analysis that we should observe is that only one of the partition functions depends on the system volume. The partition functions from the internal energy modes do not have any dependence on the volume of the system; at least, not for a thermally perfect gas. So we can find the useful and expected result that

$$p = MRT\left(\frac{\partial(\ln Q_{tr})}{\partial V}\right)_T = MRT\left(\frac{1}{V}\right) \quad .$$

This is obviously consistent with the macroscopic result.

Table 4.1 Characteristic rotational and vibrational temperatures of some common molecules.

Substance	Θ_r, °K	Θ_v, °K
H_2	87.5	6320
HD	65.8	5500
D_2	43.8	4490
HCl	15.2	4330
HBr	12.2	3820
N_2	2.89	3390
CO	2.78	3120
NO	2.45	2745
O_2	2.08	2278
Cl_2	0.351	814
Br_2	0.116	465
I_2	0.0537	309

For reference, the characteristic rotational and vibrational temperatures of some common molecules are given in Table 4.1.[11] In general, the heavier the molecule, the lower the characteristic temperatures.

The vibrational mode is really the important one for hypersonic flows. In general, for an n-atom molecule, there are multiple vibrational modes. If the structure is linear, there are $m = 3n - 5$ modes, and if the structure is nonlinear, there are $m = 3n - 6$ if the structure is non-linear. As usual, a simplifying assumption is made that the various vibrational modes are independent. This allows us to write

$$\epsilon_{vib} = \sum_{i=1}^{m} h\nu_i(v_i + \frac{1}{2}) \quad .$$

Since we have assumed the modes to be independent, we can immediately write the vibrational partition function as the product of the partition functions for the individual modes as

$$Q_{vib} = \prod_{i=1}^{m} Q_{vibi} = \prod_{i=1}^{m} \frac{1}{1 - e^{-\theta_{vi}/T}} \quad .$$

The specific heat at constant volume can then be written as

$$c_v = \frac{5}{2} + \sum_{i=1}^{m} \left(\frac{\theta_{vi}/2T}{\sinh\left(\theta_{vi}/2T\right)} \right)^2 \quad .$$

This means that there is considerably greater heat capacity in the triatom than in the the diatom.

Before introducing the topic air chemistry, it is useful to consider first the case of an adiabatic, inviscid, 1-D flow through a normal shock wave. The reason for doing this is to demonstrate the progression of caloric imperfection through internal energy excitation followed by chemical reaction. This, in fact, describes the real situation, since the rapid heating of diatomic molecules at a shock wave involves collisionally pumping the molecular population up through the vibrational levels to dissociation. In the literature, this is vibrational-dissociation coupling.

Consider a stationary normal shock, where region 1 refers to the gas upstream of the shock and region 2 refers to the gas downstream of the shock. For this case, the jump conditions at the shock can be written in the following form

$$\frac{u_2}{u_1} = \frac{\rho_1}{\rho_2} = \rho_{12}$$

$$\frac{p_2}{p_1} = 1 + \frac{\rho_1 u_1^2}{p_1}(1 - \rho_{12}) = p_{21}$$

$$\frac{h_2}{h_1} = 1 + \frac{u_1^2}{2h_1}(1 - \rho_{12}^2) = h_{21} \quad .$$

Assuming that the conditions of the gas stream are known upstream of the shock, then the unknowns are the conditions of the downstream flow, u_2, p_2, ρ_2, h_2.

For a thermally perfect gas, the equation of state is the familiar $p = \rho RT$. In addition, $h = h(T)$ only. Adding T_2 to the list of unknowns, there are now 5 equations for the 5 unknown gasdynamic variables in region 2.

Case 1. Calorically Perfect Gas

For the case of a calorically perfect gas, $h = c_p T$, and c_p = a constant. Taking the first case of a diatomic molecule at room temperature and ignoring the vibrational contribution for the moment, then the value of the specific heat derived from translational and rotational contributions is $c_p = (7/2)R$. The assumption of constant c_p requires that the shock be not too strong. Using the upstream Mach number as the independent variable, one can make use of the relations,

$$M_1 = \frac{u_1}{\sqrt{\gamma RT_1}} = \frac{u_1}{\sqrt{\gamma p_1/\rho_1}} \quad ,$$

where γ has the perfect gas value of 7/5. Using these relations in the jump equations yields (Eqs. 3.14 - 3.16):

$$\rho_{21} = u_{12} = \frac{(\gamma+1)M_1^2}{(\gamma-1)M_1^2 + 2} \quad ,$$

$$p_{21} = 1 + \frac{2\gamma}{(\gamma+1)}(M_1^2 - 1) \quad ,$$

$$h_{21} = T_{21} = 1 + \frac{2(\gamma-1)(\gamma M_1^2 + 1)}{(\gamma+1)^2 M_1^2}(M_1^2 - 1) \quad ,$$

For this case all the variables can be calculated from a knowledge of the upstream temperature and flow speed. If the shock is very strong ($M_1 >> 1$), the density jump approaches the following limiting value,

$$\frac{\rho_2}{\rho_1} = \frac{\gamma+1}{\gamma-1} \quad .$$

For a diatomic gas with constant $\gamma = 7/5$ this limiting density ratio is 6. (Of course, a strong shock will violate the assumption that the specific gas is constant!)

Case 2. Thermally Perfect, Calorically Imperfect Gas

This case is more realistic, and permits the analysis of stronger shocks for practical gases than the first case. As with the first case, the gas is still considered to be thermally perfect and a diatomic. However, the temperature rise across the shock wave is sufficient to promote vibrational excitation. Owing to this excitation, the enthalpy is

$$\frac{h_2}{RT_2} = \frac{7}{2} + \frac{\theta_v/T_2}{e^{\theta_v/T_2} - 1} \quad .$$

With this additional complication, the solution must be found iteratively. If the upstream condition is still that of a perfect gas $h_1 = 7RT_1/2$, then the enthalpy ratio across the shock will be

$$h_{21} = T_{21} + \frac{2}{7}\frac{\theta_v/T_1}{e^{\theta_v/T_2} - 1} \quad .$$

A general iterative approach is to find the downstream parameters from the jump relations of the perfect gas case after choosing a value of ρ_{12}, and then computing a corrected enthalpy based on the equation above, using also $T_{21} = p_{21}\rho_{12}$. This is repeated until everything converges.

To illustrate the trends from this approach, representative curves are shown in Fig. 4.10, where the results for the calorically imperfect jump conditions are all normalized by their perfect gas results as a function of the upstream Mach number M_1. These calculations were done for air at $T_1 = 293$ K, and we can see that the departure from ideal gas behaviour occurs near $M_1 = 2$ and the difference grows with increasing Mach number. As the Mach number increases, more of the translational energy goes into excitation of the internal energy modes of the gas, which means less energy is available for translation downstream. This means that the temperature rise across the shock is less for a calorically imperfect gas than for an ideal gas, as we see on the figure. The reduced temperature rise causes an increase in the density rise across the shock. If we now think back to the case of a hypersonic vehicle bow shock, we see that this increase in density is offset by a decrease in flow area to conserve mass, and this is the mechanism by which the shock moves closer to the body for hypersonic flight.

When M_1 is greater than 6 or 7, air becomes more active chemically, and it begins to dissociate. At this point some method is needed to predict the chemical composition of any gas as it begins to dissociate. There are at least two approaches to take for this, and both lead to the same result: the *law of mass action*. The first approach may be more familiar, since it is done through classical thermodynamics. This approach is examined first because it provides a useful illustration of how the energies of molecules and their constituent atoms are related. The second approach is a statistical mechanical approach that follows the same general approach that was used in evaluating caloric imperfection in gases.

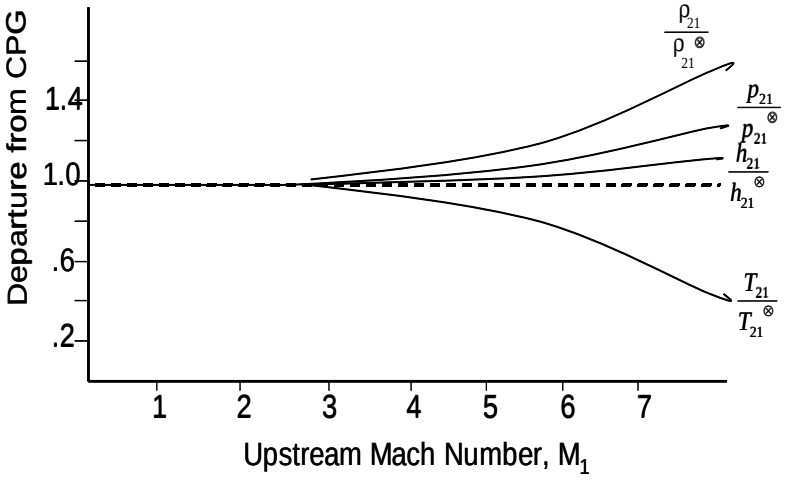

Fig 4.10. The effect of caloric imperfection on thermodynamic property ratios across a normal shock.

5. Aerothermochemistry Fundamentals

Chemical Thermodynamics

To simplify the approach, we consider the case of thermal and mechanical equilibrium. There are no unbalanced forces in the system and all species are at the same temperature as the surroundings. Moreover, the species populations follow a Boltzmann distribution for their internal energy levels. The state of the system is characterized by the $p, T, V, \eta_1, \eta_2, ..., \eta_L$, where the η_s are the species mole numbers. These thermodynamic variables are related by Dalton's law of partial pressures, which is

$$pV = \eta R_u T = \sum_s \eta_s^* R_u T = \sum_s \eta_s R_u T \quad ,$$

for a thermally perfect gas. This equation actually applies to both chemical equilibrium in the first form, where the equilibrium values of the mole numbers are denoted by the η^*, and non-equilibrium, where the instantaneous values of the mole numbers are used. The total energy and entropy of the system for the general case are

$$E = \sum_s \eta_s \hat{e}_s(T) \quad \text{and} \quad S = \sum_s \eta_s \hat{s}_s(T) \quad ,$$

where the $\hat{e}$ and $\hat{s}$ denote the energy and entropy on a per mole basis. This designation will be used explicitly throughout the analysis.

For a general chemical reaction involving the species X_s, we have the following expression

$$\alpha_1 X_1 + \alpha_2 X_2 + ... + \alpha_j X_j \rightleftharpoons \beta_{j+1} X_{j+1} + ... + \beta_L X_L \quad ,$$

where the α and β values represent the signed stoichiometric coefficients of the reaction, which are negative by convention on the LHS of the equation and positive on the RHS. To simplify the notation we define general stoichiometric coefficients as

$$\nu_s = +\beta_s \quad \text{(RHS)} \quad \text{and} \quad \nu_s = -\alpha_s \quad \text{(LHS)} \quad .$$

We define a degree of advancement of a reaction as $d\xi$ and note that the change in mole number for each species as the reaction advances is given by

$$\frac{d\eta_s}{\nu_s} = d\xi \quad .$$

As an example, it is of interest to know the amount of energy required to dissociate one mole of a molecular species to form 2 moles of the atom. The reaction can be written as $N_2 \rightarrow 2N$. Also recall that the conservation of energy can be expressed as

$$dH = dQ + V dp \quad ,$$

and we are interested in finding $Q = \int_1^2 dH = H_2 - H_1$ at constant pressure where the system enthalpy at each condition is $H = \sum_s \eta_s \hat{h}_s(T)$. For the molecule $H_1 = \hat{h}_{N_2}$ and for the dissociated atoms $H_2 = 2\hat{h}_N$. The enthalpy is related to the energy of each species by the relation

$$\hat{h}_s = \hat{e}_s + R_u T \quad ,$$

where $\hat{e}_N = (3/2)R_u T$ for the atom and $\hat{e}_{N_2} = (5/2)R_u T$ for the molecule (assuming that $T << \theta_v$). Using these values, the heat required to dissociate one mole of N_2 is

$$Q = 2\left(\frac{5}{2}R_u T\right) - \frac{7}{2}R_u T = \frac{3}{2}R_u T \quad .$$

This energy is too small, so there is something incorrect in the approach that ignores the amount of energy in the chemical bond.

The amount of energy that was not considered is equal to the dissociation energy, and we see that we cannot take an arbitrary zero point for both atoms and molecules to calculate their enthalpies. In fact, we choose to take the atom energy as the common zero point, and then subtract the dissociation energy, which is known from spectroscopic measurements, from the enthalpy of the molecule. This convention is illustrated in Fig. 5.1, which shows an arbitrary diatom potential curve (energy vs. internuclear spacing), with the energies of the atoms and molecules noted. The enthalpy for the parent molecule is now

$$\hat{h}_{N_2} = \frac{7}{2}R_u T - N_A D_{N_2} \quad ,$$

where N_A is Avogadro's number, and D_{N_2} is the dissociation energy per molecule. The amount of heat required to dissociate one mole of N_2 is now

$$Q = \frac{3}{2} R_u T + N_A D_{N_2} \quad ,$$

which is much more reasonable. To understand the relative energy in each term, we can define a characteristic temperature of dissociation as $\theta_D = D/k$, where k is Boltzmann's constant. Then $N_A D_{N_2} = R_u \theta_D^{N_2}$ and we have $Q = R_u((3/2T + \theta_D^{N_2})$. For nitrogen, the characteristic dissociation temperature is on the order of 113,000 K.

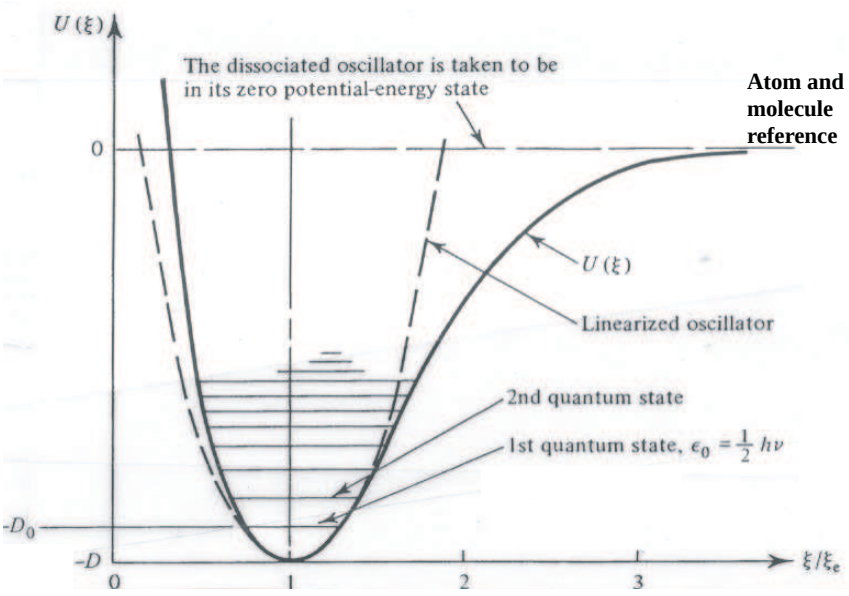

Fig. 5.1. Energy reference point for molecules and atoms.

The difference in energy is the bond energy, or dissociation energy. Finally, we note that the amount of heat calculated above is the amount of heat required for one unit of advancement of the reaction, so in general we can write

$$\left(\frac{dQ}{d\xi}\right)_{p,T} = \sum_s \nu_s \hat{h}_s \equiv \Delta \hat{H} \quad ,$$

where $\Delta \hat{H}$ is the *heat of reaction.* This can be derived more formally by noting that

$$dQ_{p,T} = dH = \sum_s d\eta_s \hat{h}_s(T) \quad .$$

If both sides are divided by $d\xi$, and then we can write

$$\left(\frac{dQ}{d\xi}\right)_{p,T} = \sum_s \frac{d\eta_s}{d\xi} \hat{h}_s = \sum_s \nu_s \hat{h}_s \quad ,$$

since by definition $d\eta_s = \nu_s d\xi$.

Law of Mass Action

To shorten this process, we will start the derivation from the Gibbs equation, but we will discuss both the concept of entropy maximization and Gibbs free energy minimization. Recall from thermodynamics that the Gibbs equation is

$$TdS = dE + pdV - \sum_s \hat{\mu}_s d\eta_s \quad ,$$

where all terms have been defined previously except the chemical potential, $\hat{\mu}_s$. For a chemically reacting system, there are two contributions to entropy; those into or out of the system (by heat transfer, for example) and from internal production via chemical reaction. Therefore, the differential entropy is

$$dS = d_e S + d_i S \quad \text{where} \quad d_e S = \frac{dQ}{T} \quad \text{and} \quad d_i S \geq 0 \quad .$$

The first law of thermodynamics can be written as $dQ = dE + pdV$, and this can be substituted into the Gibbs relation to give

$$TdS = dQ - \sum_s \hat{\mu}_s d\eta_s \quad .$$

If we consider the case of an adiabatic flow, then

$$TdS = -\sum_s \hat{\mu}_s d\eta_s \geq 0 \quad .$$

Finally, the relation between the stoichiometric coefficients and the change in species mole numbers, $d\eta_s = \nu_s d\xi$, can be used to derive the constraint that

$$\sum_s \hat{\mu}_s \nu_s d\xi \leq 0 \quad ,$$

based on the internal production of entropy by chemical reaction. From this result we can infer that a necessary condition for chemical equilibrium (without heat addition) is that the internal entropy production be 0. For finite $d\xi$, this means that also that the sum of the chemical potentials times the stoichiometric coefficients is zero.

$$\sum_s \hat{\mu}_s^* \nu_s = 0 \quad .$$

This is the equation of reaction equilibrium that is obtained from the condition of entropy maximization.

A more useful relation that describes chemical equilibrium can be derived based on the minimization of the Gibbs free energy. Recall the definition that

$$G \equiv H - TS \Rightarrow dG = dE + pdV - SdT - TdS \quad ,$$

and from the preceding analysis we can substitute for TdS using the relation given earlier to eliminate some terms on the RHS and obtain,

$$dG = -SdT - \sum_j \hat{\mu}_j d\eta_j \quad .$$

If we specify conditions of constant pressure and temperature, we obtain the result that

$$dG_{p,T} = \sum_j \hat{\mu}_j d\eta_j = \sum_j \hat{\mu}_j \nu_j d\xi \leq 0 \quad .$$

This is the same result that was obtained from the analysis of the system entropy. Again, at equilibrium $d\xi = 0$, and the same equilibrium condition, $\sum_s \nu_s \hat{\mu}_s = 0$ is also found from the analysis of the Gibbs free energy. Consequently, since entropy was maximized, the Gibbs free energy must be minimized. Furthermore, for a single species

$$\left(\frac{\partial G}{\partial \eta_s}\right)_{p,T,\eta'_s} = \hat{\mu}_s \quad ,$$

where the η'_s is used to denote that the mole numbers of the other species are kept constant. This result shows that the chemical potentials are the specific Gibbs free energies. These are on a molar basis, and they are evaluated at the conditions of the mixture. To acknowledge this, we now substitute the symbol for the specific Gibbs free energy for the chemical potential, $\hat{g}_s = \hat{\mu}_s$. The specific Gibbs free energy (gfe) can also be expressed as

$$\hat{g}_s = \hat{g}^0_s + R_u T \ln p_s \quad ,$$

where the $\hat{g}^0_s$ is the gfe for the species in its pure state ($\eta = \eta_s$) at unit pressure, and p_s is the partial pressure of species s. At equilibrium then,

$$\sum_s \nu_s \hat{\mu}^*_s = \sum_s \nu_s (\hat{g}^0_s + R_u T \ln p^*_s) = 0 \quad ,$$

which can be rearranged as follows

$$-\frac{\sum_s \nu_s \hat{g}^0_s}{R_u T} = \sum_s \nu_s \ln p^*_s = \ln \prod_s (p^*_s)^{\nu_s} \quad .$$

The latter relation can be recognized as the law of mass action, and it can be written in terms of the equilibrium constant K_p as

$$\ln \prod_s (p^*_s)^{\nu_s} = \ln K_p(T) \quad ,$$

or, simply

$$K_p(T) = \prod_s (p^*_s)^{\nu_s} \quad .$$

The equilibrium constant is also the ratio of the forward reaction rate to the backward reaction rate,

$$K_p(T) = \frac{k_f(T)}{k_b(T)} \quad .$$

The variation of the equilibrium constant is found by

$$\frac{d(\ln K_p(T))}{dT} = \frac{\Delta\hat{H}}{R_u T^2} \quad ,$$

where $\Delta\hat{H} \equiv \sum_s \nu_s \hat{h}_s(T)$ is the heat of reaction. This equation is known as the Van't Hoff equation, and it describes which way the reaction will shift if you change temperature. It can also be used to calculate $\Delta\hat{H}$ for a reaction based on the measured temperature variation of the equilibrium constant.

Examples of Air Thermochemical Reactions

At certain high temperature equilibrium conditions, there is a significant amount of NO present in a hypersonic air flow. This is important for a number of reasons. First, NO is a precursor of NO_x, which is a pollutant, and, second, it is strongly radiating species when it is thermally excited. Finally, it is also a useful species for making Laser-Induced Fluorescence measurements in high-speed flows, because it has allowed single-photon transitions that are accessible to commercially available laser systems.

To illustrate the use of the equilibrium constant, we would like to find the temperature at which there is 1000 ppm of NO in 1 atm of air that has been heated ($\chi_{NO} = .001$). The reaction of interest is,

$$\frac{1}{2}N_2 + \frac{1}{2}O_2 \rightleftharpoons NO \quad ,$$

and the equilibrium constant or this equation is

$$K_p = \frac{p_{NO}}{p_{O_2}^{\frac{1}{2}} p_{N_2}^{\frac{1}{2}}} \quad .$$

Note that for this reaction, there is no pressure dependence, since if $p_s = \chi_s p$ is substituted for each species, the pressures cancel. First, assume that the initial mole fractions are $\chi_{N_2} = .79$ and $\chi_{O_2} = .21$ and that these are constant, since $\chi_{NO} = .001$ at the final condition. From the tabulated value of $K_p(T)$[15], we find that at $T = 1000$ K, there is 35 ppm of NO, and at 1500 K, there is 1320 ppm of NO from this reaction. So 1000 ppm is reached at about 1400 K. The dependence on temperature is exponential, and at 2500 K, there would be 24000 ppm of NO, and the assumption that it is a minor species in the mole fraction balance breaks down. However, there is another mechanism that limits the peak NO concentration to less than this value.

The single isolated reaction considered above is not representative of air thermochemistry. As the temperature reaches 2000 K at 1 atm pressure the oxygen molecules begin to dissociate by the reaction

$$O_2 \rightleftharpoons 2O \quad ,$$

which has the equilibrium constant,

$$K_p = \frac{p_O^2}{p_{O_2}} \quad .$$

If this reaction is included in the analysis of the NO generation, we find that the NO concentration peaks near 10000 ppm at a temperature of 2500 K, which is lower than the concentration expected from the single reaction analysis alone. Including the oxygen dissociation in the analysis also brings in a pressure dependence, since for this reaction

$$K_p = \frac{p_O^2}{p_{O_2}} = \left(\frac{\chi_O^2}{\chi_{O_2}}\right) p \quad ,$$

or

$$\frac{K_p(T)}{p} = \frac{\chi_O^2}{1-\chi_O} \quad .$$

Increasing pressure decreases the oxygen dissociation and this would affect the peak value of NO.

This illustrates the difficulty involved in accurately accounting for even the equilibrium thermochemistry of air. As temperature increases, more reactions and species must be considered, and the bookkeeping must be carefully done. There are some common sources of equilibrium air compositions and properties. There is the old stand-by publication, NACA TN 4265, by Moeckel and Weston, [12] and there is the CEA code by Gordon and McBride [13]. At VKI, there is now the PEGASE library [14], which includes equilibrium chemical composition to high temperatures.

Statistical Mechanical Derivation of K_p

To complete the analysis and relate it back to the statistical mechanical description that has proven to be a useful way of evaluating macroscopic thermodynamic quantities, the derivation of the law of mass action from the evaluation of the most probable macrostate is briefly described. Consider, for example, the reaction above for oxygen dissociation and assume that the macrocsopic quantities, energy, volume and total oxygen atom number density, E, V, N_O, are given. Then we again make arbitrary arrangements of the groupings of energy levels, their populations, and their energies for both species $(C_j^{O_2}, N_j^{O_2}, \epsilon_j^{O_2}; C_j^O, N_j^O, \epsilon_j^O)$ and then use these quantities to find the most probable macrostate. The assumption that the macrostate probabilities are independent of each other is made, so that $W = W^{O_2}(N_j^{O_2}) W^O(N_j^O)$, which gives $\ln W = \ln W^{O_2} + \ln W^O$. In addition, as with the general case for a single species, the results are obtained in the Boltzmann limit. The procedure is then to maximize $\ln W$, subject to the constraints that

$$N_O = 2\sum_j N_j^{O_2} + \sum_j N_j^O \quad ,$$

and

$$E = \sum_j N_j^{O_2}(\epsilon_j^{O_2} - D^{O_2}) + \sum_j N_j^O \epsilon_j^O \quad .$$

The dissociation energy accounts for the energy in the chemical bond. The system of equations can be solved using the method of Lagrange multipliers, and by eliminating the undetermined multipliers from the results. For the case of a dissociating homonuclear diatomic molecule, this yields

$$\frac{(N^O)^2}{N^{O_2}} = \frac{(Q^O)^2}{Q^{O_2}} e^{-D/kT} \quad .$$

This is the law of mass action for a dissociating diatom, and it can be written in terms of partial pressures for a thermally perfect gas as

$$\frac{p_O^2}{p_{O_2}} = K_p(T) = \frac{kT}{V} \frac{(Q^O)^2}{Q^{O_2}} e^{-D/kT} \quad ,$$

showing explicitly the temperature dependence mentioned above. Using this equation, it is possible to calculate an equilibrium composition from information about the energy levels of species. Of course, the accuracy of the approach depends on the accuracy of the partition functions, and the simplified analytical expressions of the previous section are not sufficient for this purpose.

Ionizing Gases - Saha Equation

To complete the description of equilibrium air thermochemistry, one should also consider the case of an ionizing single-atom species,

$$O^+ + e^- \rightleftharpoons O \quad ,$$

and for simplicity, only single ionization is considered. This reaction is exactly analagous to the case of a dissociating molecule, so the law of mass action for an ionizing atom is

$$\frac{N^O}{N^{e^-} N^{O^+}} = \frac{Q^O}{Q^{e^-} Q^{O^+}} e^{I/kT} \quad .$$

The only difference is that the ionization energy, I, replaces the dissociation energy. To simplify the equation, it is convenient to write the populations in terms of one component, and this is done by noting that $N^{O^+} = N^{e^-}$, or that the charge in the system is neutral. Also, the total number of O atoms is constant, so $N^{O^+} + N^O = (N^O)_0$, where $(N^O)_0$ is the original number of O atoms in the system. Finally, a degree of ionization is defined as

$$\phi = \frac{N^{O^+}}{(N^O)_0} \quad .$$

Inverting the original expression for the ionizing law of mass action and noting that $(N^O)_0 = \rho V / m_O$, it can be rewritten in terms of the degree of ionization as

$$\frac{\phi^2}{1-\phi} = \frac{m_O}{\rho V} \frac{Q^{e^-} Q^{O^+}}{Q^O} e^{-\theta_I/T} \quad .$$

The characteristic ionization temperature has been defined as $\theta_I = I/k$. For each of the species, the partition functions can be written as

$$Q^s = Q^s_{trans} \prod_{int} Q^s_{int} \quad .$$

The only internal energy for the electron is associated with its spin, which has two degenerate states at zero energy, so $Q^e_{int} = 2$. The translational partition function for the electron is

$$Q^e_{trans} = V \left(\frac{2\pi m_e kT}{h^2} \right)^{\frac{3}{2}} \quad .$$

For the ionizing specie, the masses of the ion and neutral are nearly equal, since the only difference is in the mass of an electron, so there translational partition functions will effectively cancel. With these relations, the expression for the degree of ionization can be written as

$$\frac{\phi^2}{1-\phi} = \frac{m_O}{\rho} \left(\frac{2\pi m_e kT}{h^2} \right)^{\frac{3}{2}} \frac{2 \prod_{int} Q^{O^+}_{int}}{\prod_{int} Q^O_{int}} e^{-\theta_I/T} \quad .$$

To express the equation in terms of pressure and temperature,note that

$$pV = (N^{e-} + N^O + N^{O^+})kT = (1+\phi)kT/m_O \quad ,$$

and this finally give

$$\frac{\phi^2}{1-\phi^2} = \frac{1}{p} \left(\frac{2\pi m_e}{h^2} \right)^{\frac{3}{2}} (kT)^{\frac{5}{2}} \frac{2 \prod_{int} Q^{O^+}_{int}}{\prod_{int} Q^O_{int}} e^{-\theta_I/T} \quad .$$

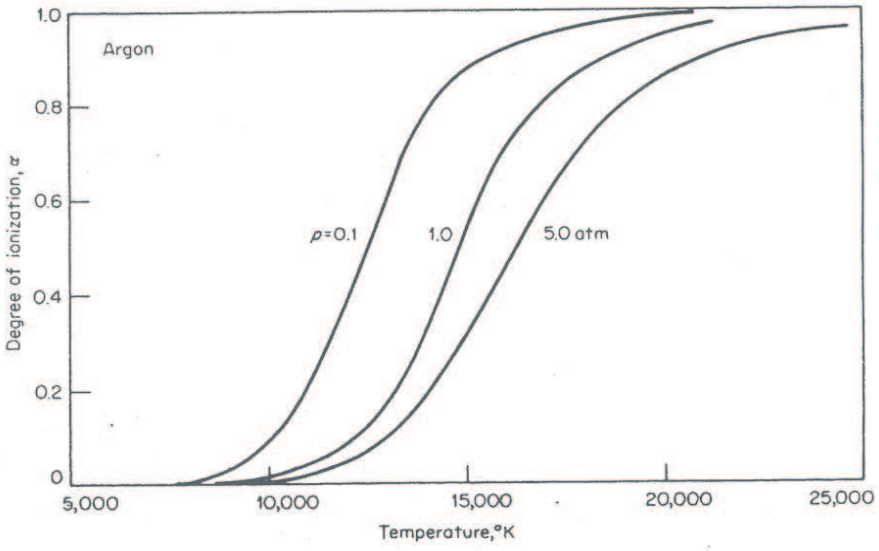

Fig. 5.3 Equilibrium ionization of argon as a function of temperature and density [16].

Either of these two equations can be called the Saha equation, and there are a number of other forms as well. However, it will usually be presented in much simpler form for

atomic species, which have only electrical contributions to the internal energy. If excitation in the ground level of the neutral and the ion are ignored, and if the temperature is reasonable, then the partition functions are constants, and the equation can be written as

$$\frac{\phi^2}{1-\phi^2} = \frac{CT^{5/2}}{p} e^{-\theta_I/T} \quad .$$

Using the law of mass action, it is possible to calculate the degree of ionization for any species as a function of temperature and pressure. This is done for argon in Fig. 5.3, where the three curves show the degree of ionization at various pressures as a function of temperature. Note that as pressure is decreased, the ionization fraction at constant temperature increases.

Nonequilibrium

For situations where the gas is not in equilibrium, one can distinguish between two different cases for both chemical and thermal nonequilibrium. The general definitions are given below, and the parameter that determines which case applies to a given situation for chemical nonequilibrium is the Damkohler number $Da = \tau_F/\tau_C$. A similar nondimensional parameter can be defined for an energy transfer process, and this can be used to assess nonequilibrium situations for thermal processes, such as vibrational energy transfer.

Chemical Nonequilibrium: mixture composition is changing with time at a fixed location or in space at a fixed time. Distinctions are made for three different situations:

a. *Near equilibrium* – $Da >> 1$ – small departure from equilibrium, and inconsequential.
b. *Nonequilibrium* – $Da \approx 1$ – the general case where the composition is changing. Usually, the collision rate between particles is not sufficient to complete the reactions, but enough collisions are occurring that the mixture composition continues to change.
c. *Frozen* – $Da << 1$ – the mixture composition is no longer changing because there is not enough time to allow sufficient inter-particle collisions for reactions to go to completion. Although the mixture composition does not change, it does not correspond to the equilibrium mixture for the local pressure and translational temperature. This can happen for example in a rapid expansion of a high-enthalpy gas, where pressure drops so quickly that there are not enough collisions to complete the reactions.

For thermal nonequilibrium the same situations can occur as with chemical nonequilibrium, and we can therefore distinguish the following situations:

a. *Near equilibrium* – there are sufficient collisions between particles to equilibrate the populations in all of the energy modes at a common temperature.
b. *Nonequilibrium* – the energy distribution is changing or evolving and the collisions are not sufficient to reach equilibrium, but are frequent enough to continue to transfer energy between modes.
c. *Frozen* – the energy distributions in each mode do not correspond to a single temperature, and the distributions of particles over the available energy levels can

be non-Boltzmann. We usually assume that they are still Boltzmann, although at different temperatures. This allows modeling of only the total species and the transfer processes without having to model separately the populations in each energy level (which is actually required).

Note that if the composition is frozen, it can be assumed to have a constant value of entropy from that point on, and this has been used to model frozen flow in nozzles under very high expansion ratios with some success.

The issue of nonequilibrium is particularly important for ground testing in facilities that attempt to duplicate hypersonic flight conditions. As the simulation is not perfect, the ability to interpret test results and to relate them to flight is made even more difficult by the inability to directly measure test conditions other than by spectroscopic means. Even with these approaches, the assumption of thermochemical equilibrium is often invoked to simplify the analysis. In the past, many different types of facility have been developed for hypersonic and high-enthalpy flow testing, and these are shown in a rather crude fashion in Fig. 5.4, where the range of characteristic flow time relative to chemical time is shown. Note that the continuous flow facilities do not cover much of this domain.

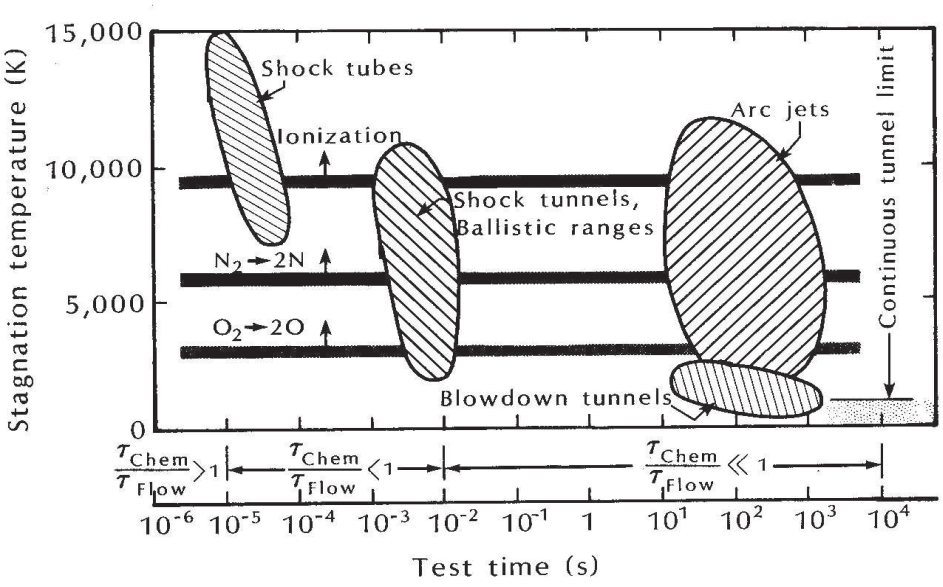

Fig. 5.4 Hypersonic ground test facilities.[3]

Recall that the total enthalpy can be considered constant, thus the stagnation temperature shown on the y axis is a measure of the total stagnation enthalpy of the facilities, and the larger values correspond to the requirement to simulate higher flight speeds (recall that $h_0 \approx u^2/2$).

6. Summary

Some of the basic principles of hypersonic flow have been presented in these lecture notes. Following a general description of the characteristic features of hypersonic flight, the basic thermodynamic and fluid dynamic considerations were reviewed for perfect gases and for imperfect gases, with particular attention to caloric imperfection. A statistical mechanics approach was used to derive analytic expressions for the thermodynamic

property variation of calorically imperfect gases. Concepts of equilibrium thermochemistry were then presented, with particular attention given to the case of a dissociating diatom and an ionizing atom. This was followed by a brief description of nonequilibrium flow situations.

Acknowledgements

The author would like to thank the Personnel of the von Karman Institute who have very kindly helped to produce these lecture notes. Special thanks go to the Library and Printing Office Staff. Additional acknowledgement is due to all of the VKI Faculty and adjunct Professors who have taught Hypersonics Seminars at one time or another, former colleagues at NASA Ames Research Center, and Prof. James McDaniel of UVa. Finally, all mistakes in these notes are uniquely the fault of the author.

References

1. J. D. Anderson Jr., Hypersonic and High Temperature Gas Dynamics, McGraw-Hill, New York, (1989).
2. H. W. Liepmann and A. Roshko, Elements of Gasdynamics, John Wiley & Sons, New York, (1957).
3. J. J. Bertin, Hypersonic Aerothermodynamics, AIAA Inc., Washington, DC, (1994).
4. Ames Research Staff, NACA, "Equations, Tables, and Charts for Compressible Flow", NACA Report 1135.
5. A. H. Shapiro, The Dynamics and Thermodynamics of Compressible Fluid Flow, John Wiley & Sons, New York, (1953).
6. R. H. Korkegi, "Hypersonic Aerodynamics", VKI Course Note 9, von Karman Institute, Rhode-Saint-Genese, (1966).
7. J. T. Howe, "Hypervelocity Atmospheric Flight: Real Gas Flow Fields", NASA Technical Memorandum 101055, June, (1989).
8. G. W. Castellan, Physical Chemistry, 3^{rd} Ed., Addison-Wesley, Reading, (1983).
9. W. G. Vincenti and C. H. Krueger Jr., Introduction to Physical Gas Dynamics, R. E. Krieger, Malabar, (1982).
10. C. F. Hanson, "Molecular Physics of Equilibrium Gases: A Handbook for Engineers", NASA Publication SP-3096, (1976).
11. C. L. Tien and D. Lienhard, Statistical Thermodynamics, McGraw-Hill, New York, (1992).
12. W. E. Moeckel and K. C. Weston, "Composition and Thermodynamic Properties of Air in Chemical Equilibrium", NACA Technical Note 4265, April, (1958).
13. S. Gordon and B. J. McBride, "Computer Program for Calculation of Complex Chemical Equilibrium Compositions and Applications I. Analysis", NASA Reference Publication 1311, (1994).
14. B. Bottin, D. Vanden Abeele, M. Carbonaro, G. Degrez, G.S.R. Sarma, "Thermodynamic and Transport Properties for Inductive Plasma Modeling", *J. Thermophysics and Heat Transfer*, **13**(3), pp. 343-350, July, (1999).
15. D. R. Stull and H. Prophet, JANAF Thermochemical Tables, Second Edition, NSRDS-NBS 37, Washington, DC, (1971).
16 . R. G. Jahn, Physics of Electric Propulsion, McGraw-Hill Book Company, New York, (1968).